# Interpreting ISR Data

Joshua Semeter, Boston University

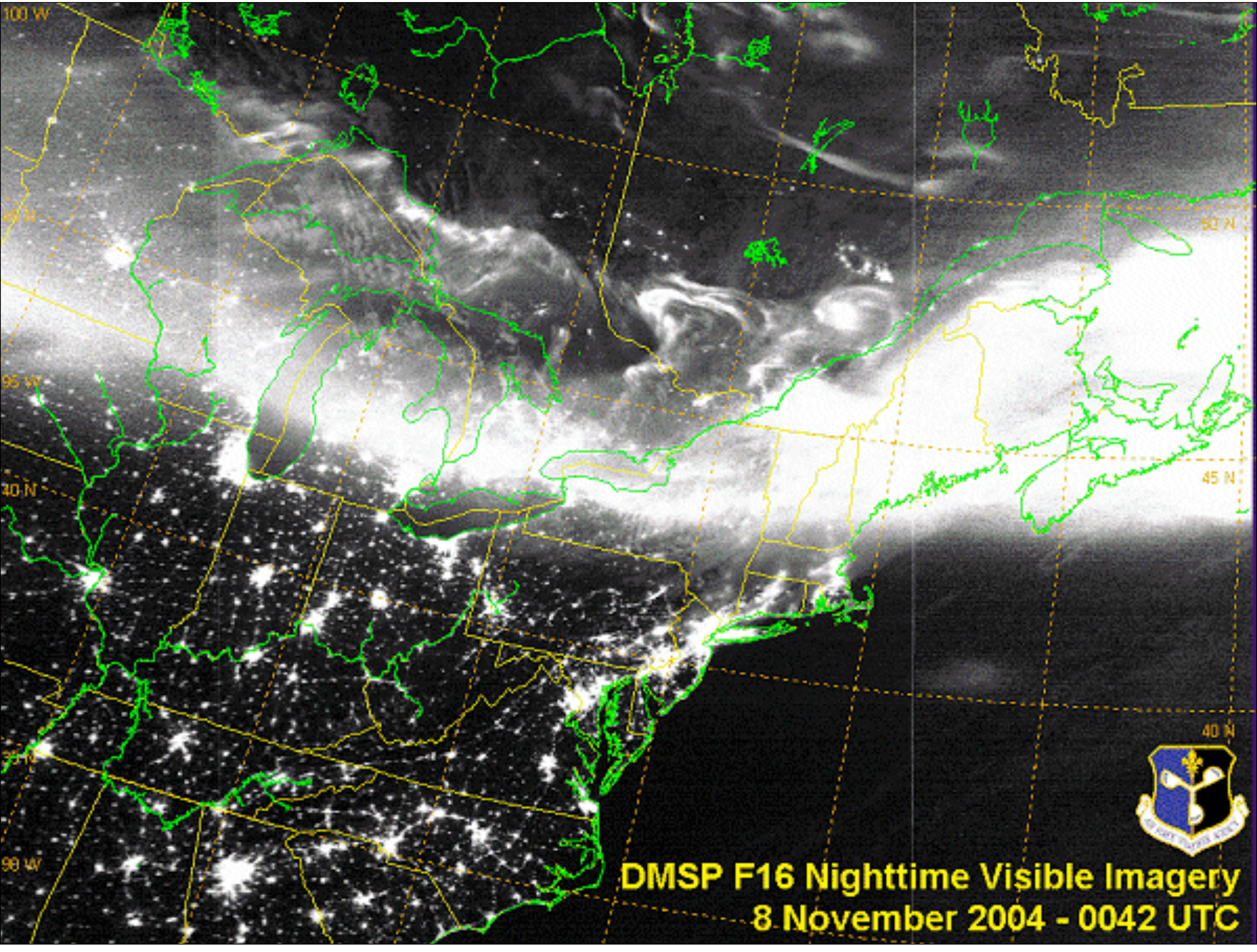
100 W
95 W
90 W
50 N
45 N
40 N
DMSP F16 Nighttime Visible Imagery
8 November 2004 - 0042 UTC

# Universal Themes

- Plasma luminescence reveals magnetic field structure.

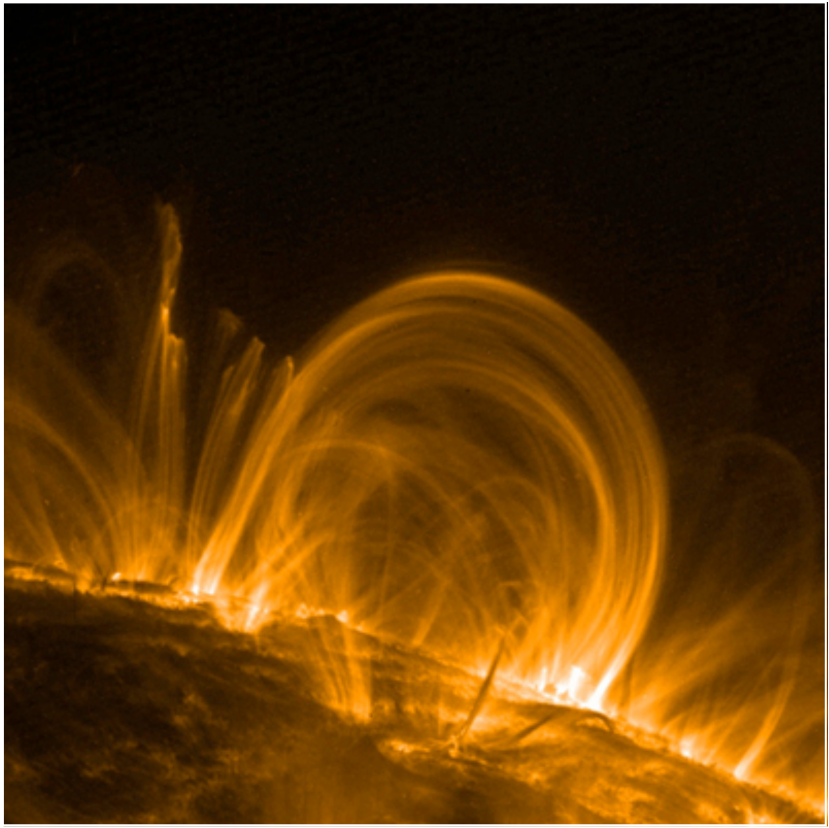

**Plasma loops**

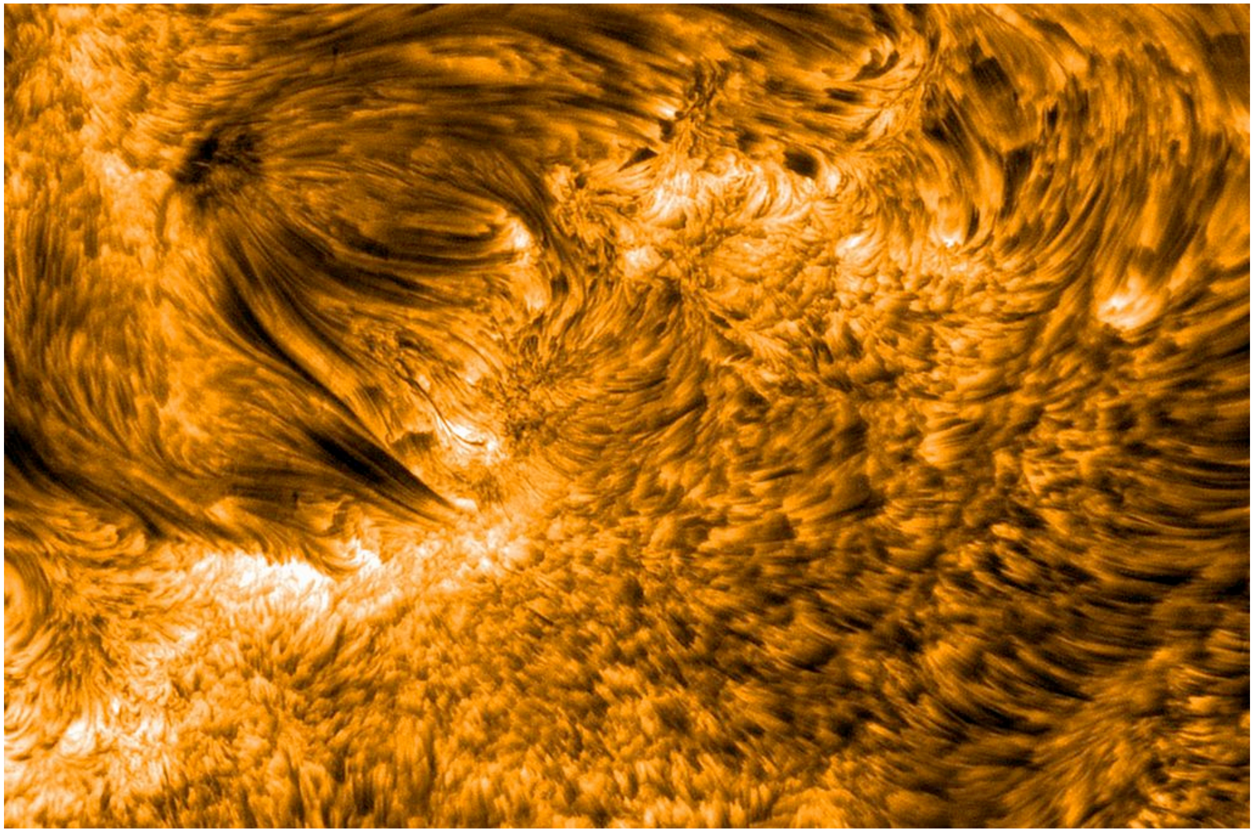

**Spicules**

171A images, 1,000,000 K

# Universal Themes

- Plasma luminescence reveals magnetic field structure.

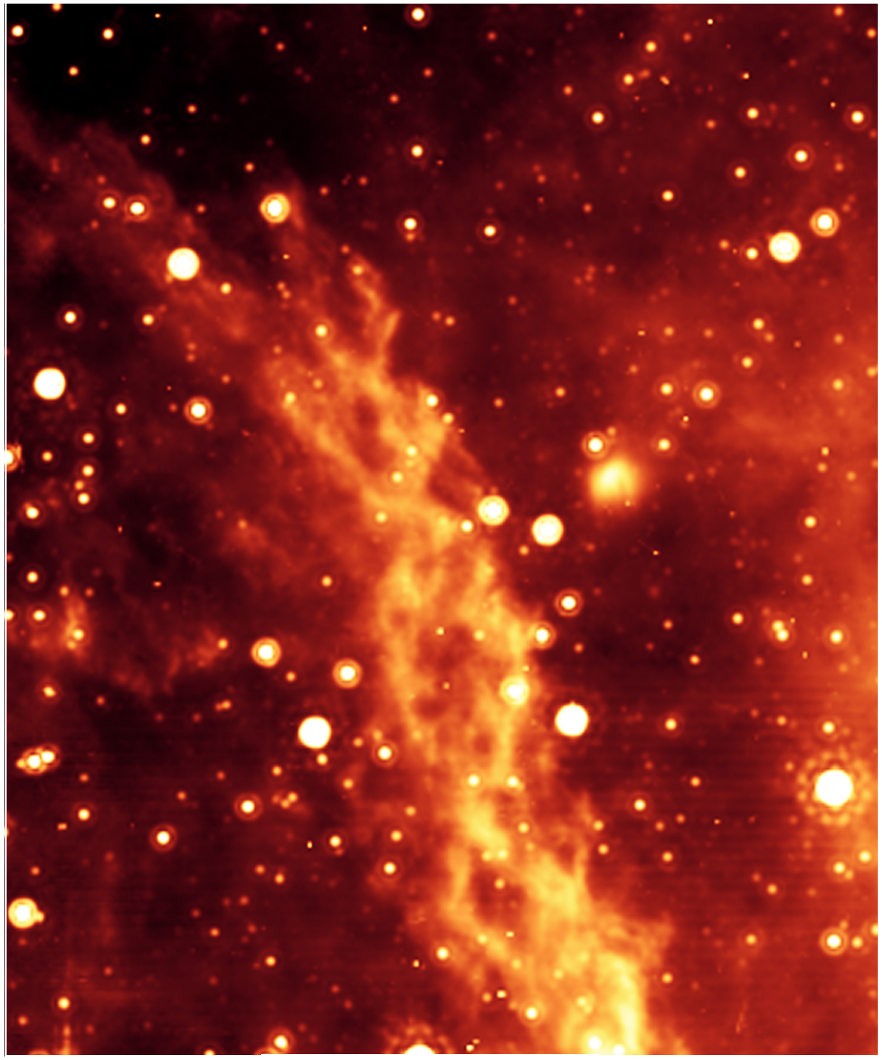

80 light years

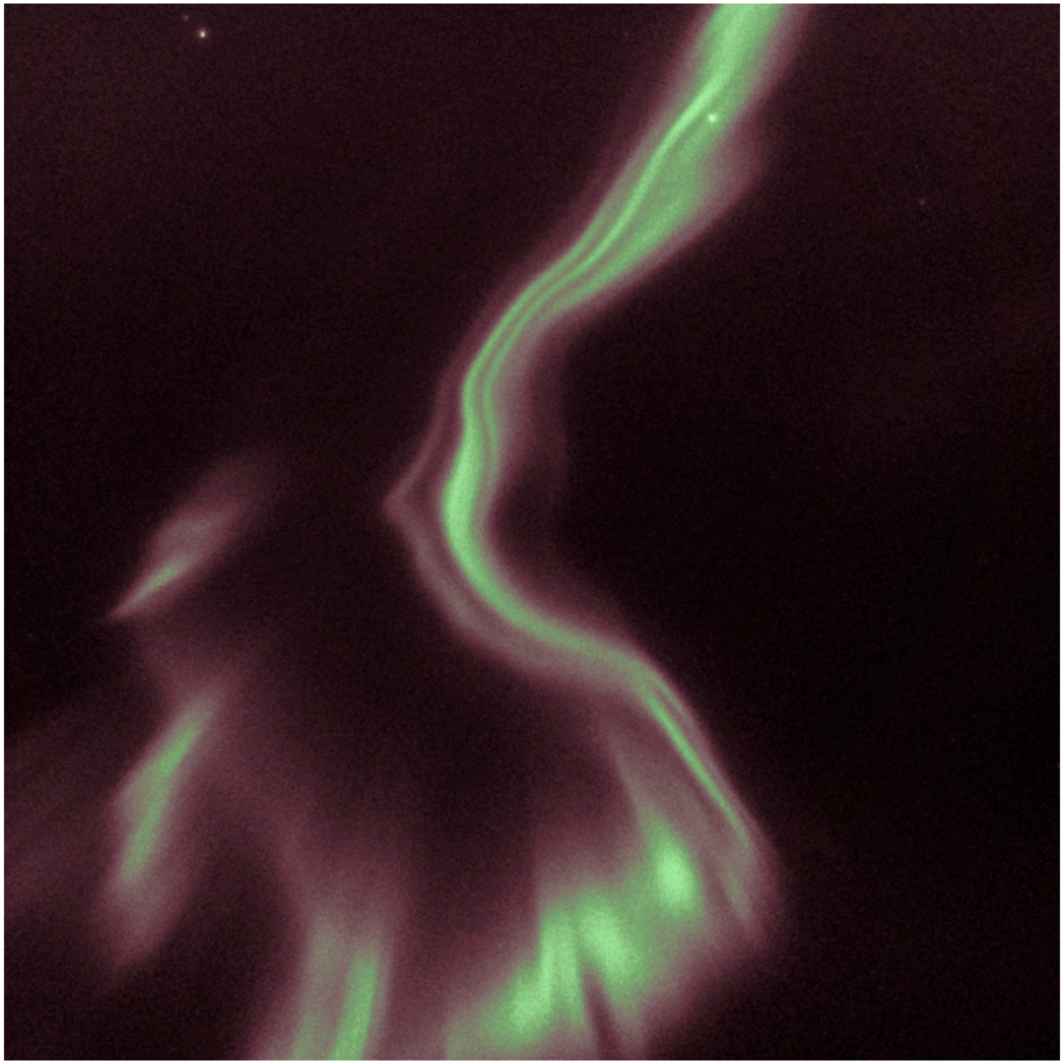

15 km

# Universal Themes

- Plasma luminescence reveals magnetic field structure.
- Explosive release of energy.

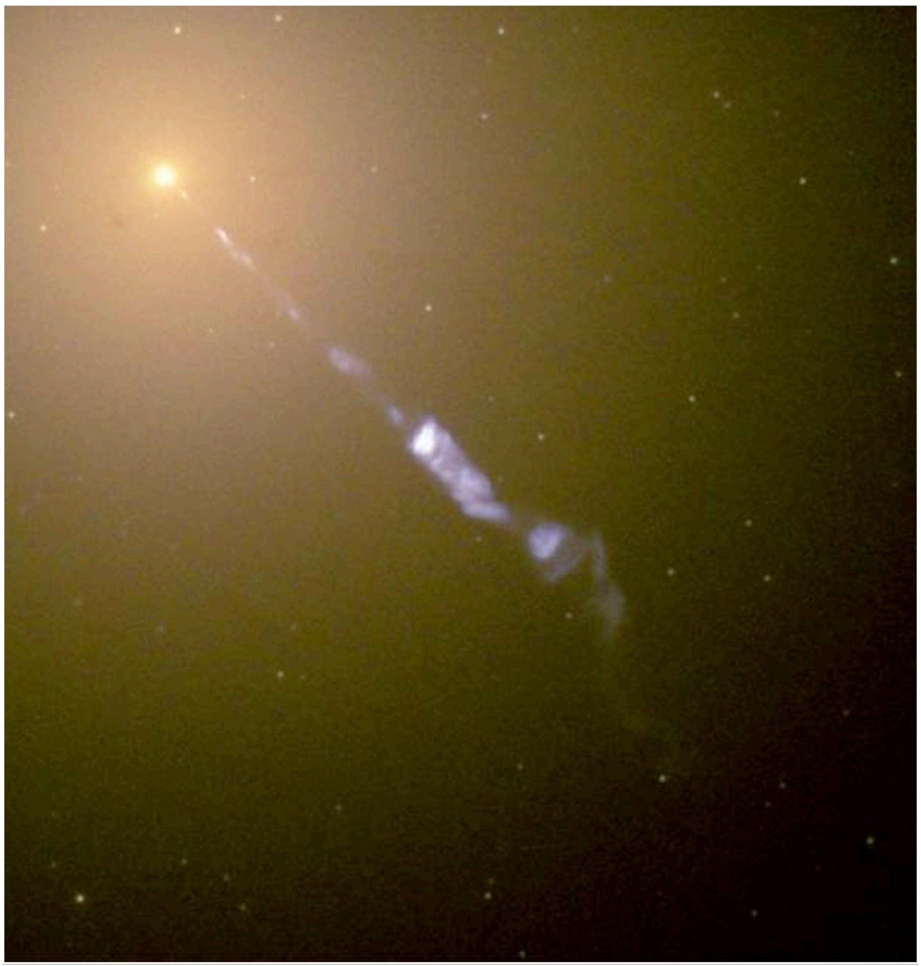

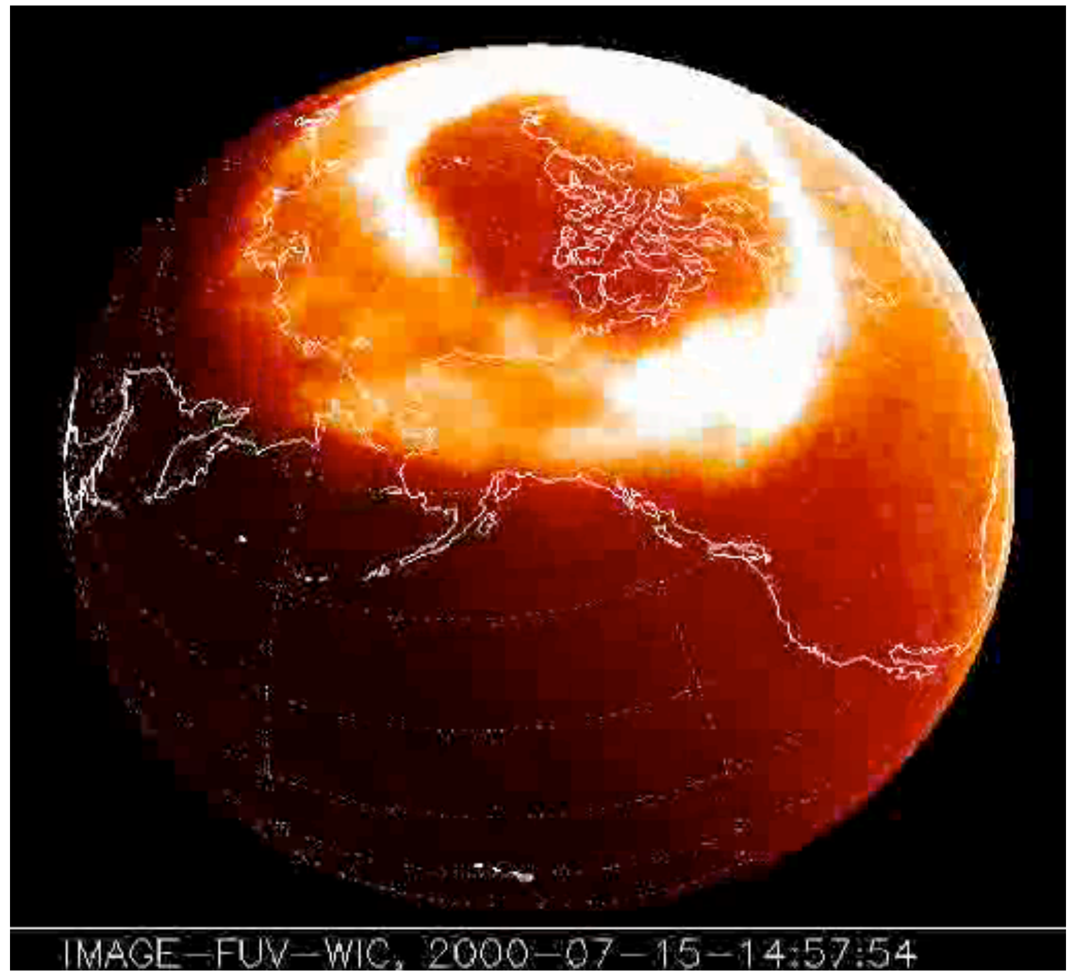

# Universal Themes

- Plasma luminescence reveals magnetic field structure.
- Explosive release of energy.
- Vorticity.

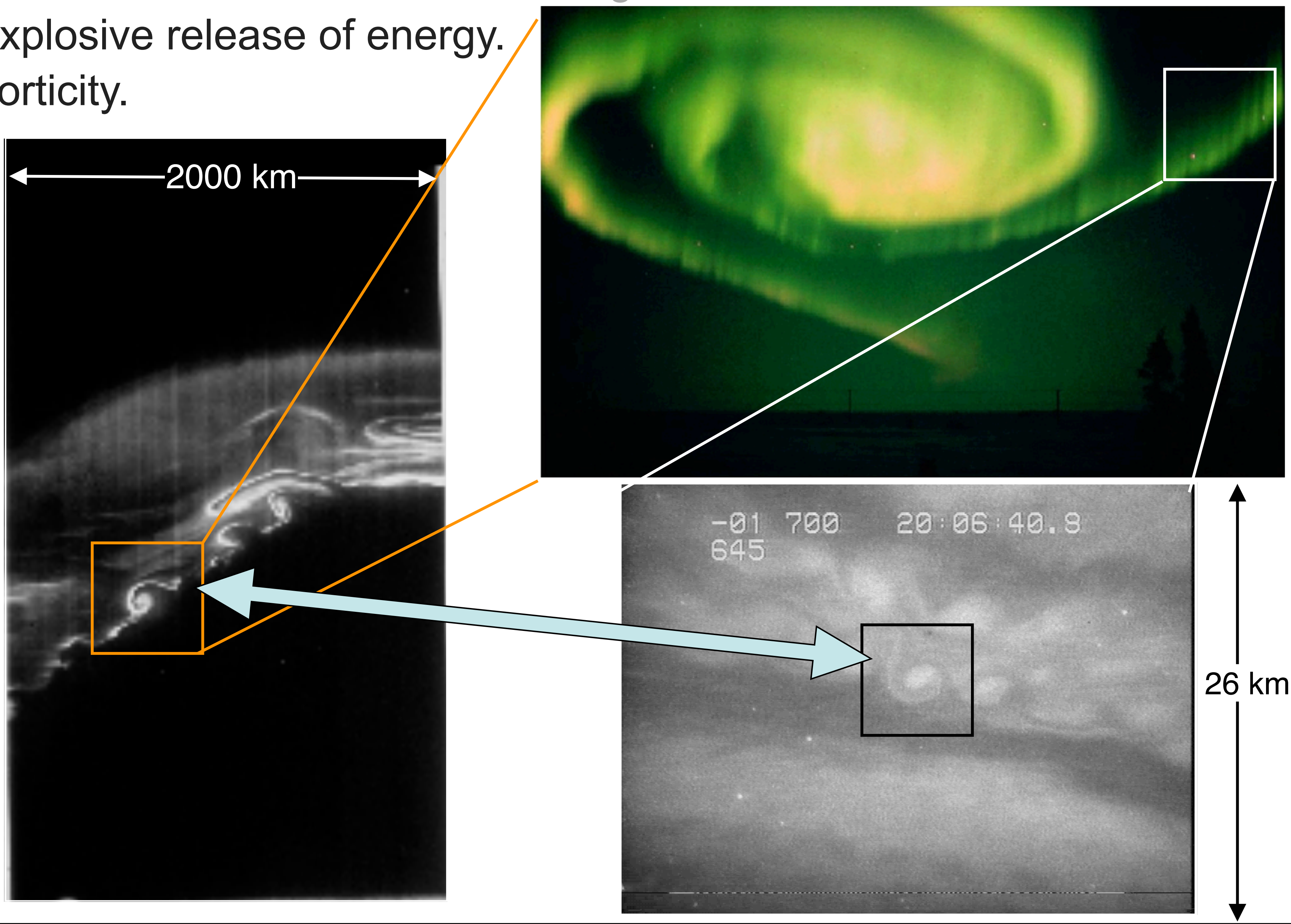

# Universal Themes

- Plasma luminescence reveals magnetic field structure.
- Explosive release of energy.
- Vorticity.
- Filamentation.

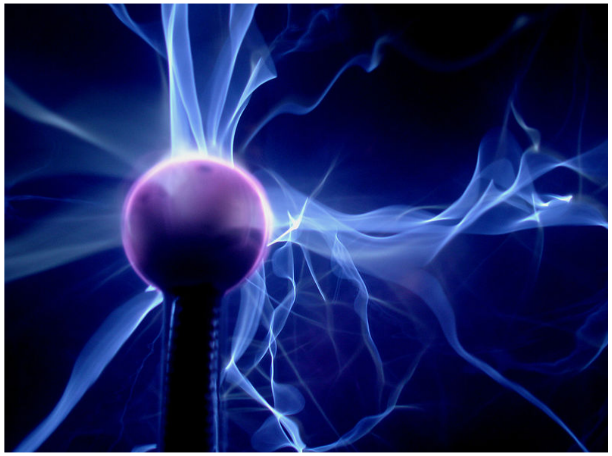

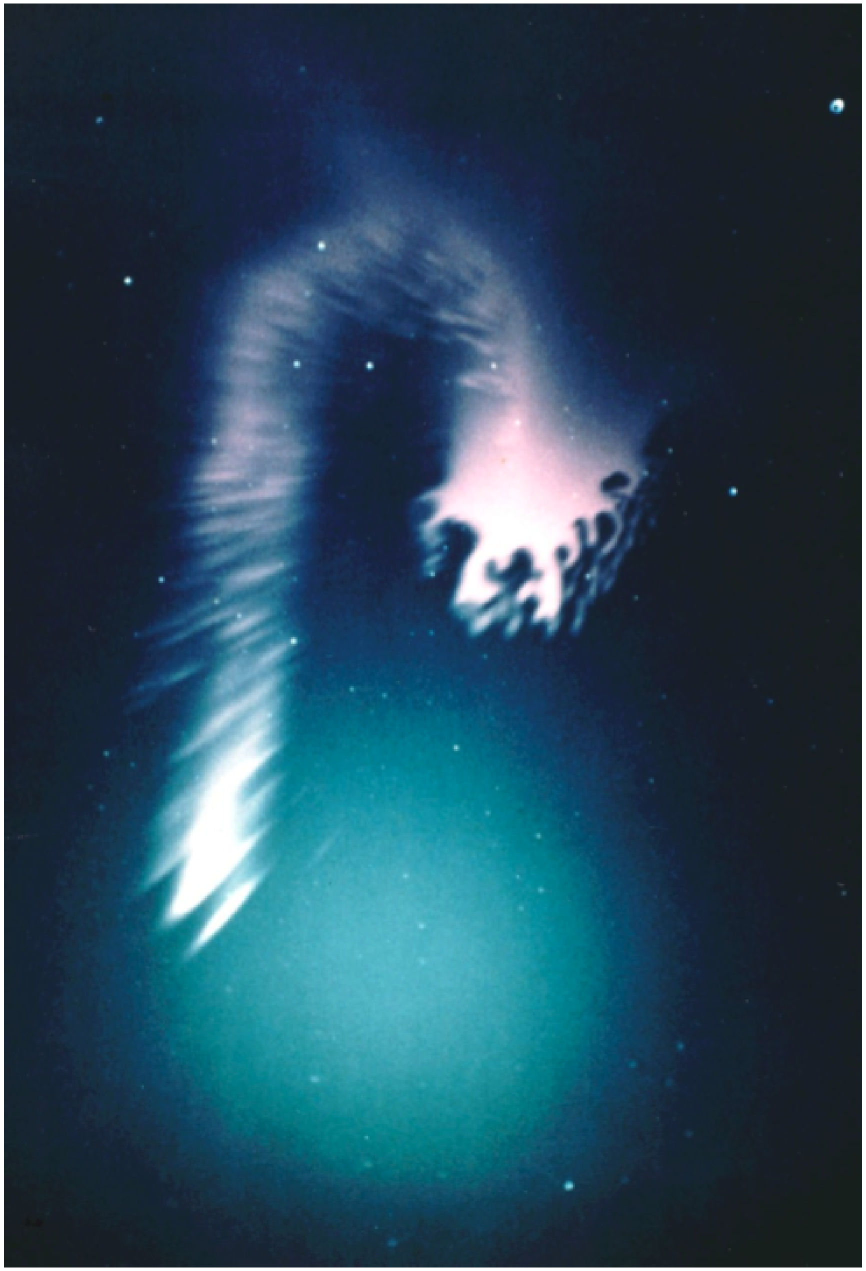

# Universal Themes

- Plasma luminescence reveals mag
- Explosive release of energy.
- Vorticity.
- Filamentation.
- Perspective.

# Universal Themes

- Plasma luminescence reveals magnetic field structure.
- Explosive release of energy.
- Vorticity.
- Filamentation.
- Perspective.
- Resolution (space, time wavelength).

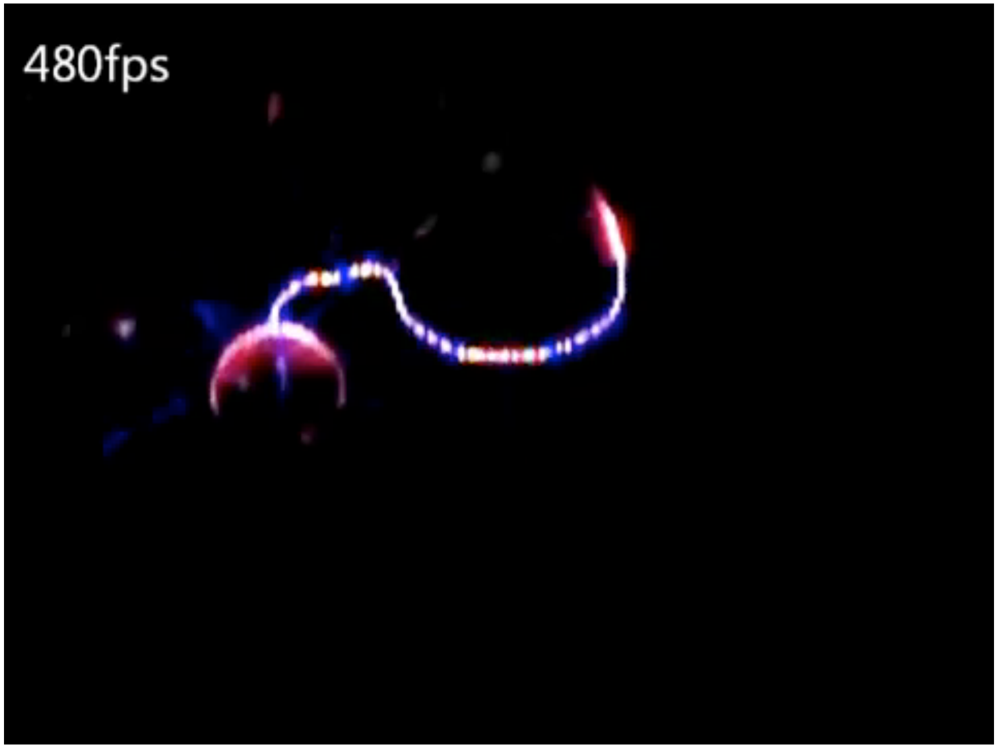


# Universal Themes

- Plasma luminescence reveals magnetic field structure.
- Explosive release of energy.
- Vorticity.
- Filamentation.
- Perspective.
- Resolution (space, time wavelength).

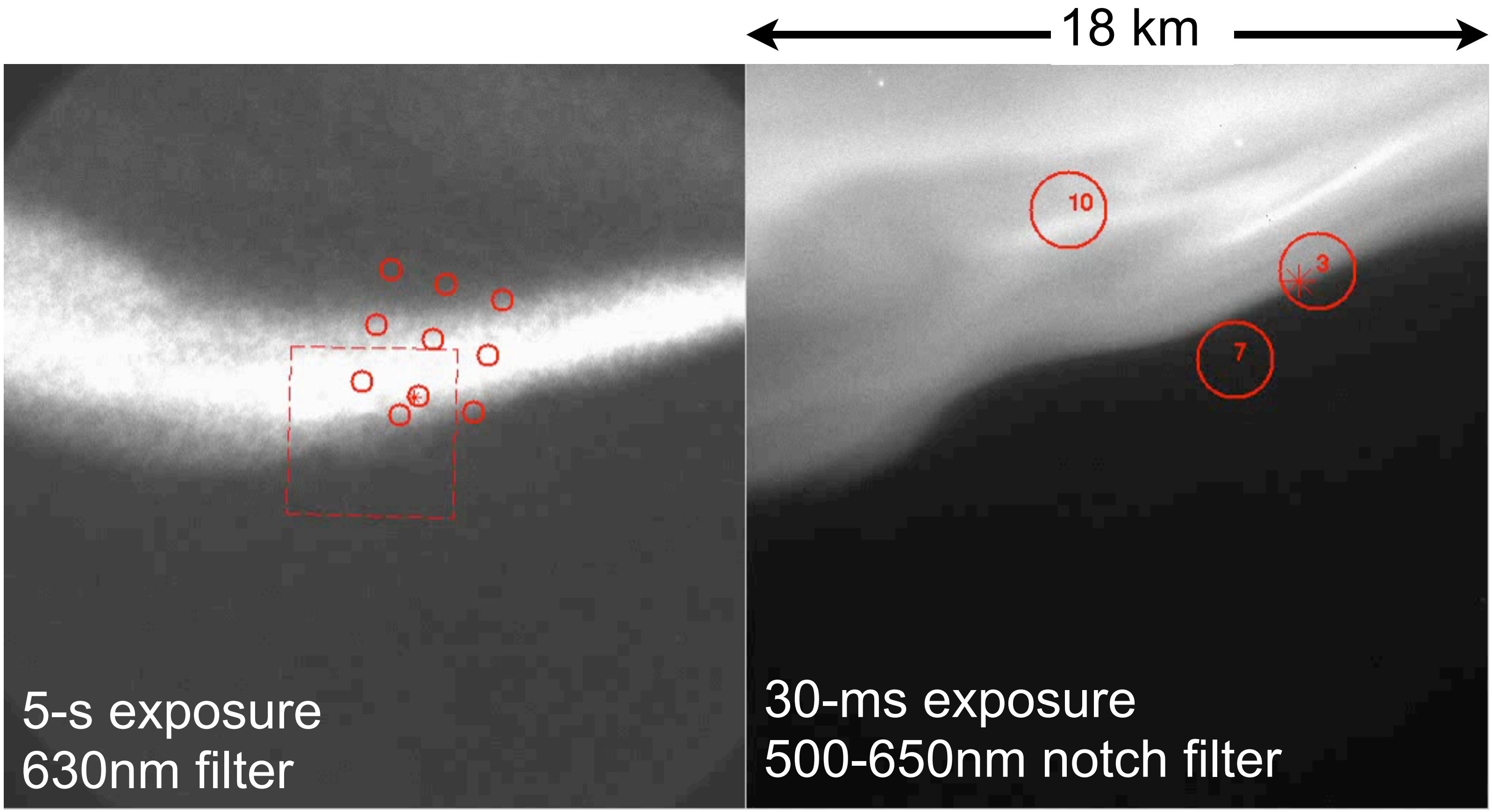

# Universal Themes

## Physics

- Plasma luminescence reveals magnetic field structure.
- Explosive release of energy.
- Vorticity.
- Filamentation.

## Engineering

- Perspective.
- Resolution (space, time wavelength).

# Solar wind - Magnetosphere Coupling: Energy Storage and Release

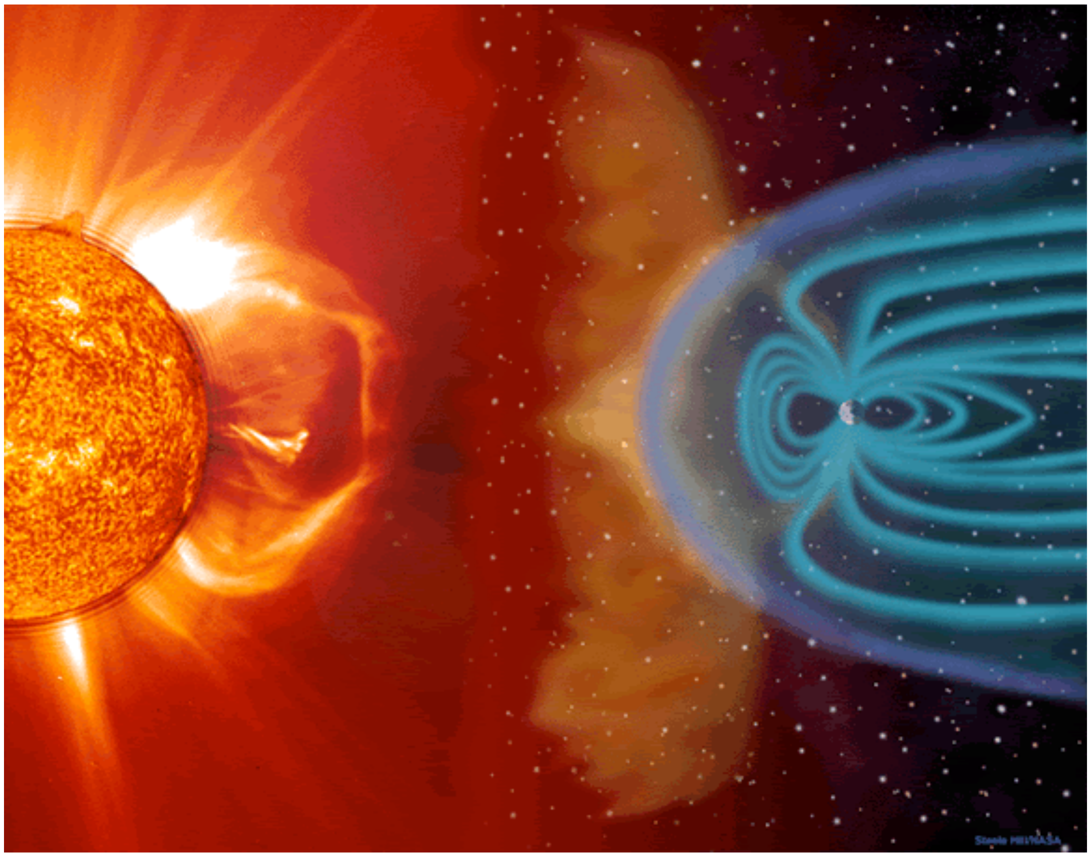

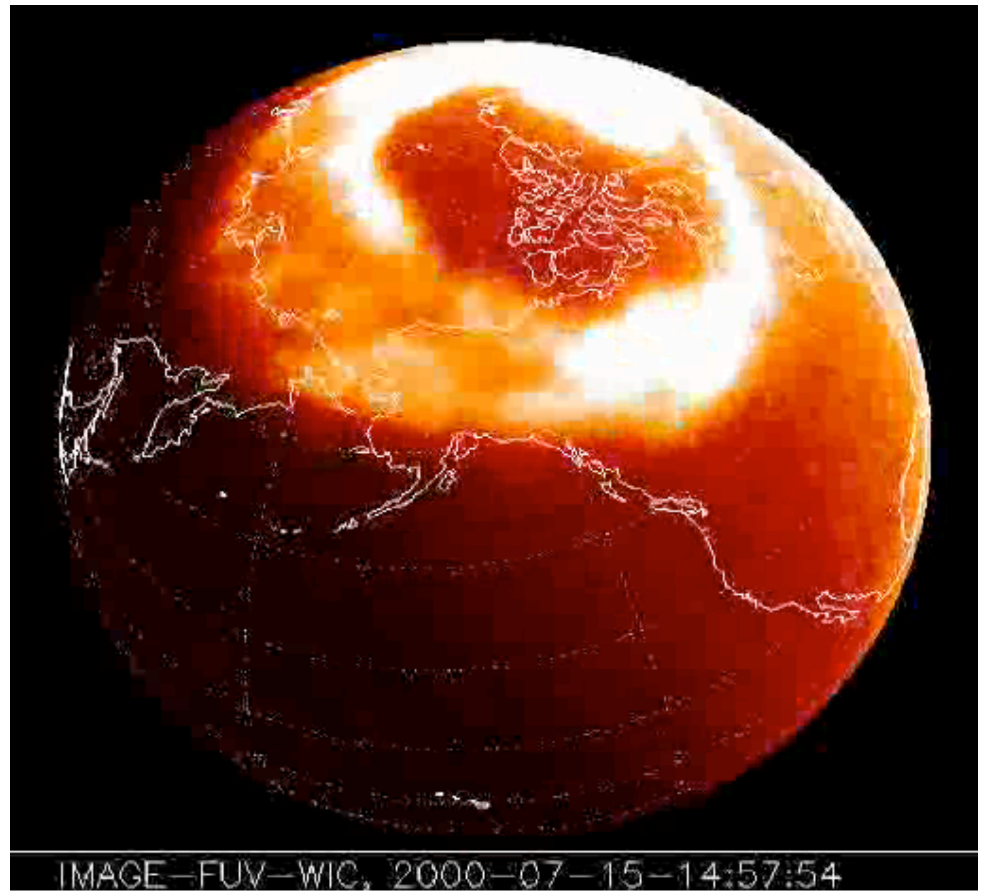

# Pixelated Planet

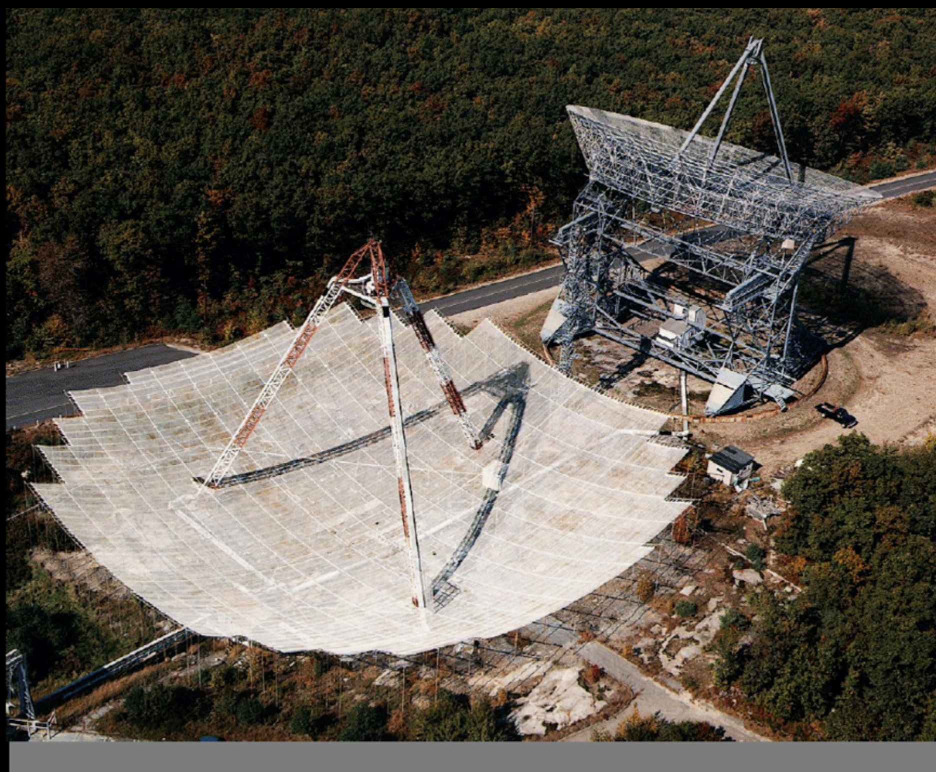

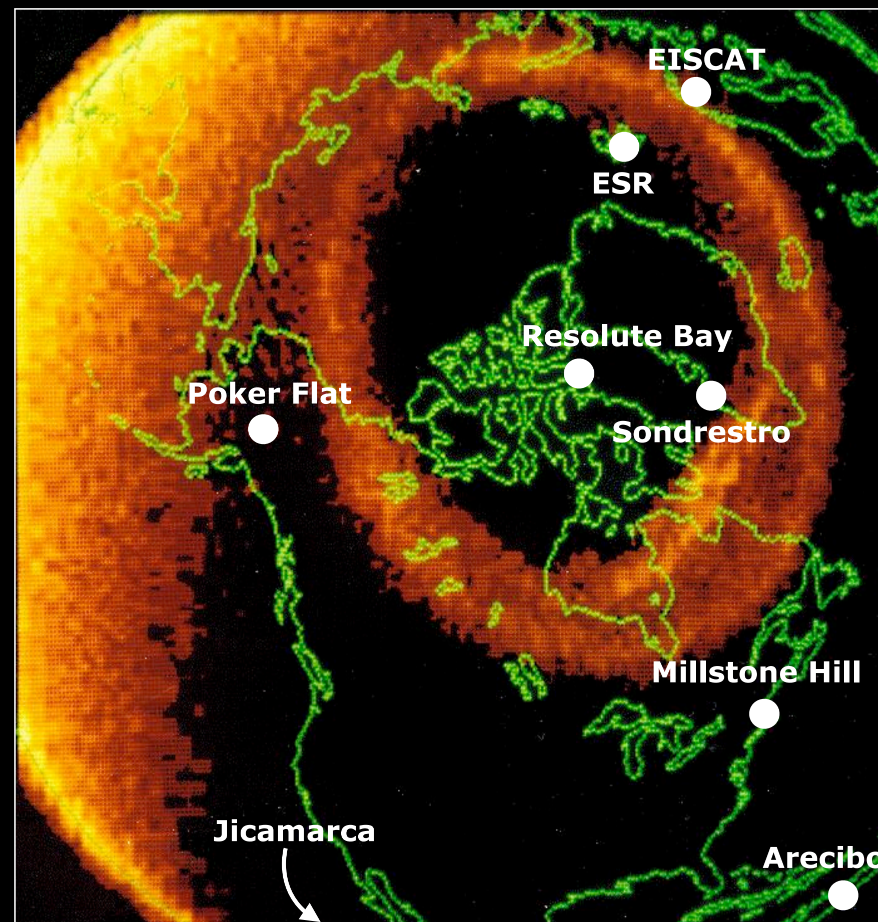

# Poker Flat Incoherent Scatter Radar (PFISR)

Poker Flat, Alaska

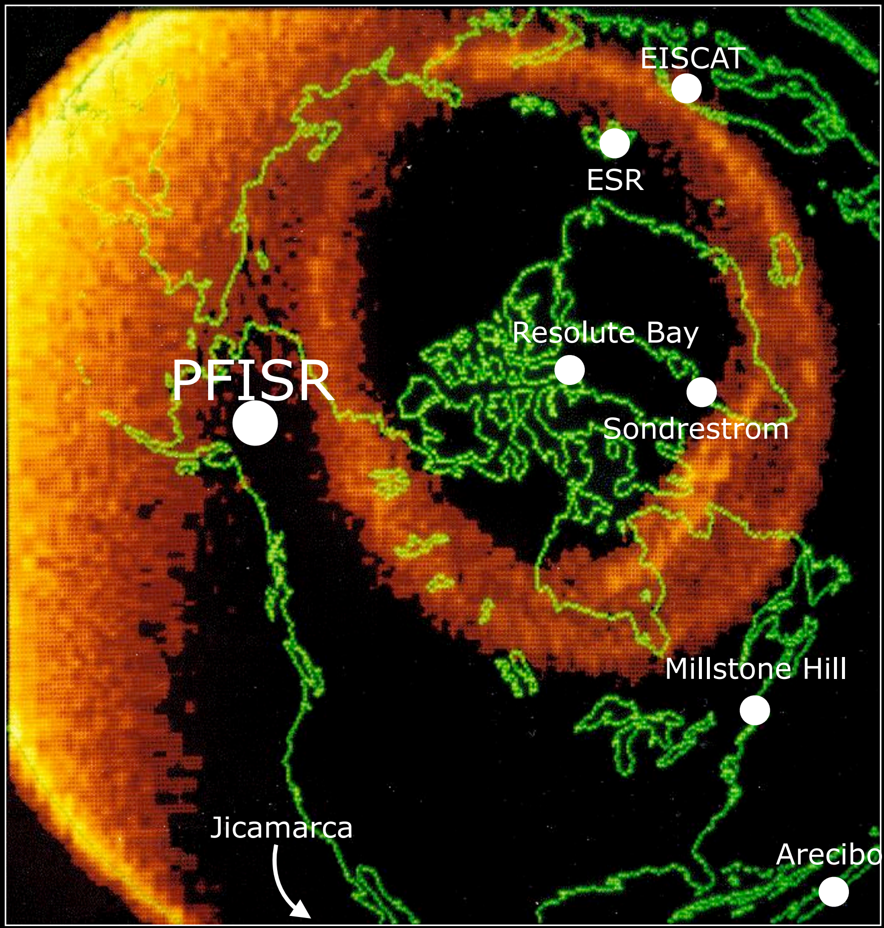

# Solar wind - Magnetosphere Coupling: Energy Storage and Release

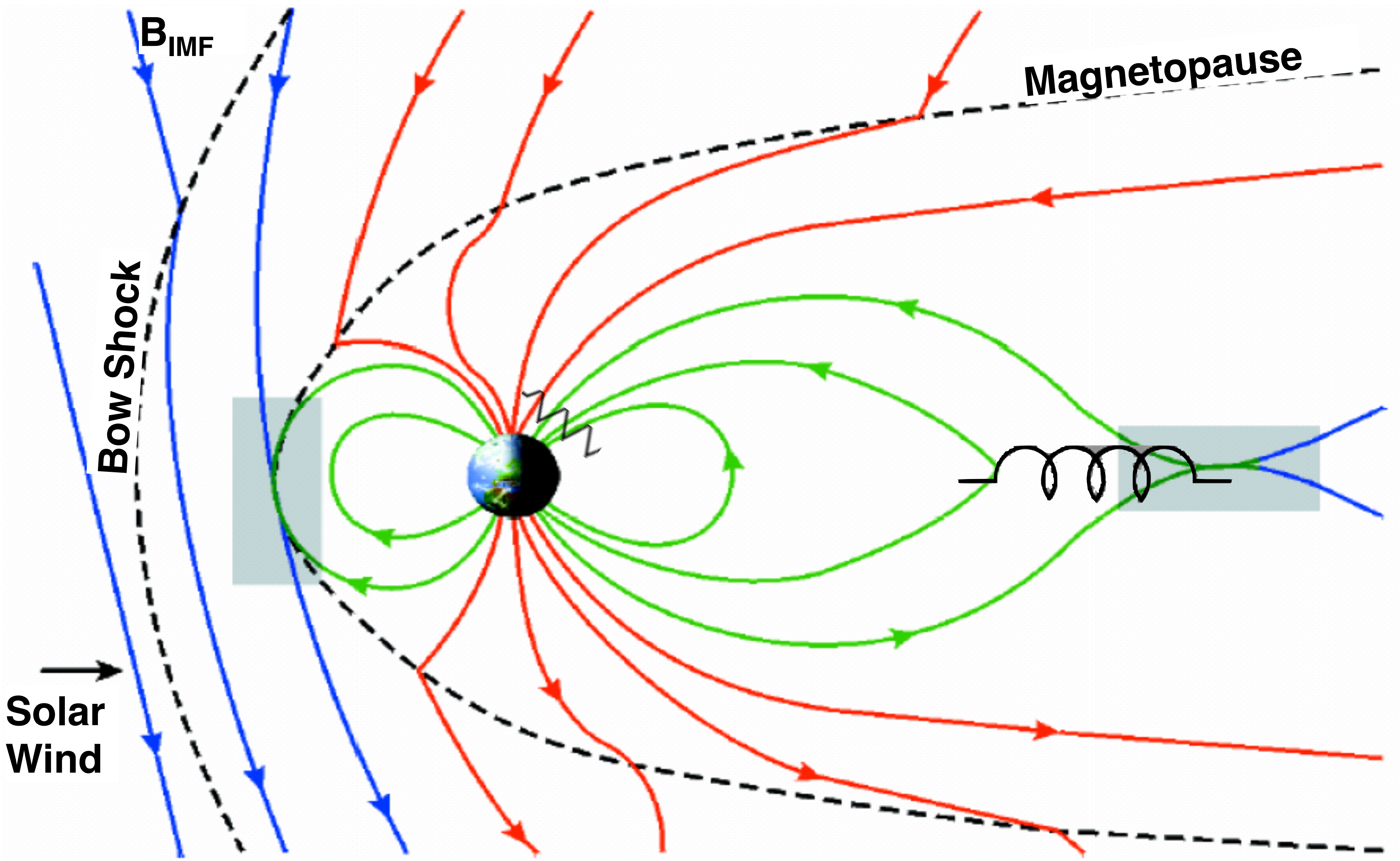

# The EMF comes from Poynting flux delivered by the magnetosphere

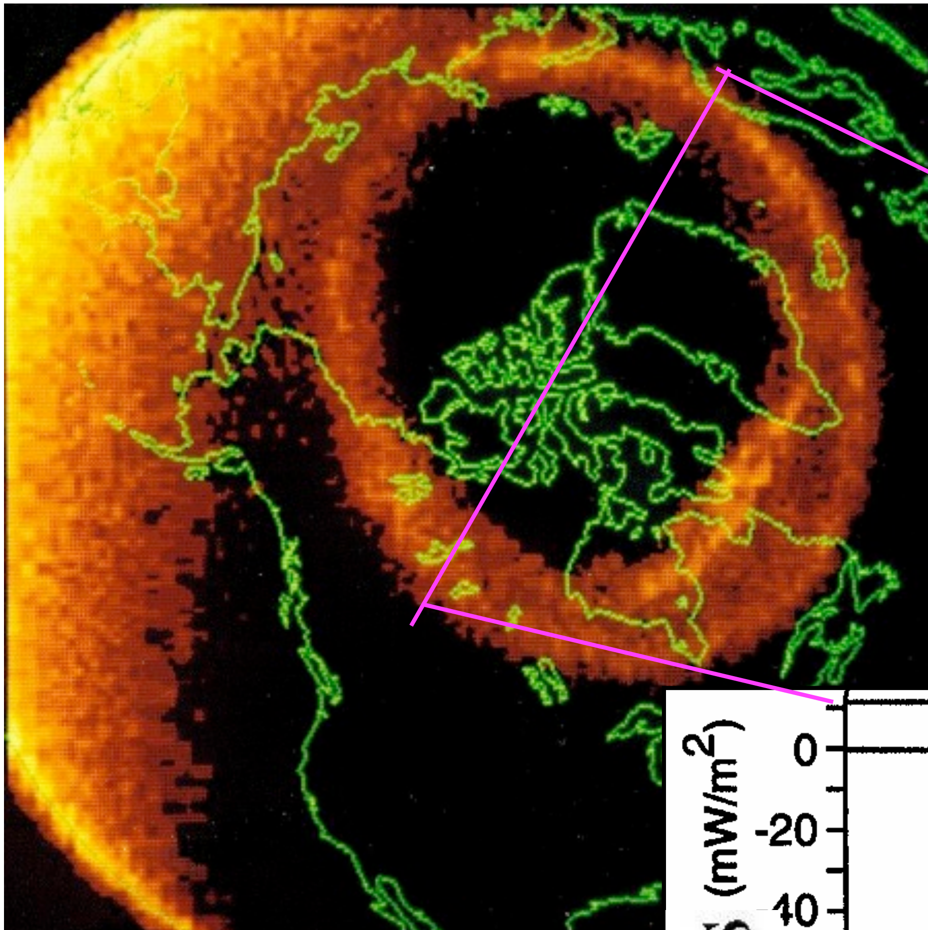

**Poynting Flux:**

$$\mathbf{S} = \frac{E \times B}{\mu_0}$$

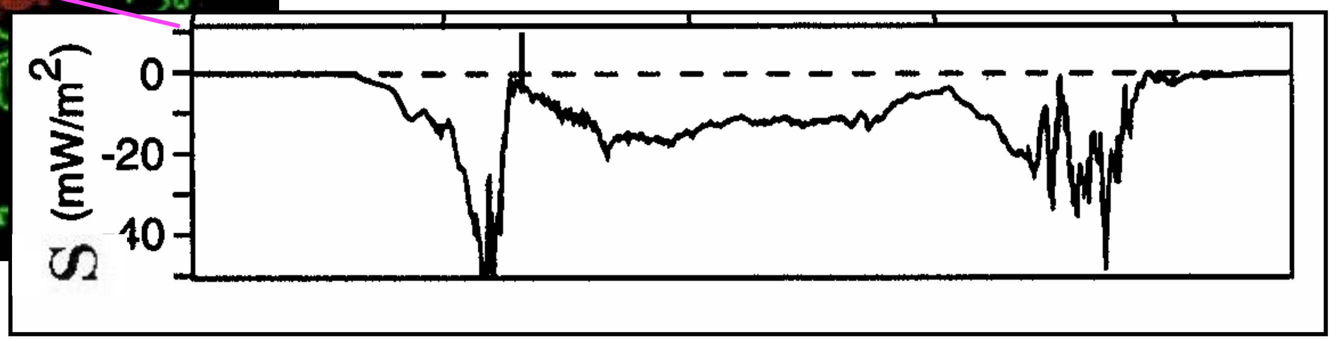


**Poynting flux is carried by magnetic field-aligned currents.**
**The currents are generated by mechanical interactions (dynamo) between the solar wind and magnetosphere.**
**The ionosphere looks like a resistive load to this current.**

# The auroral current circuit

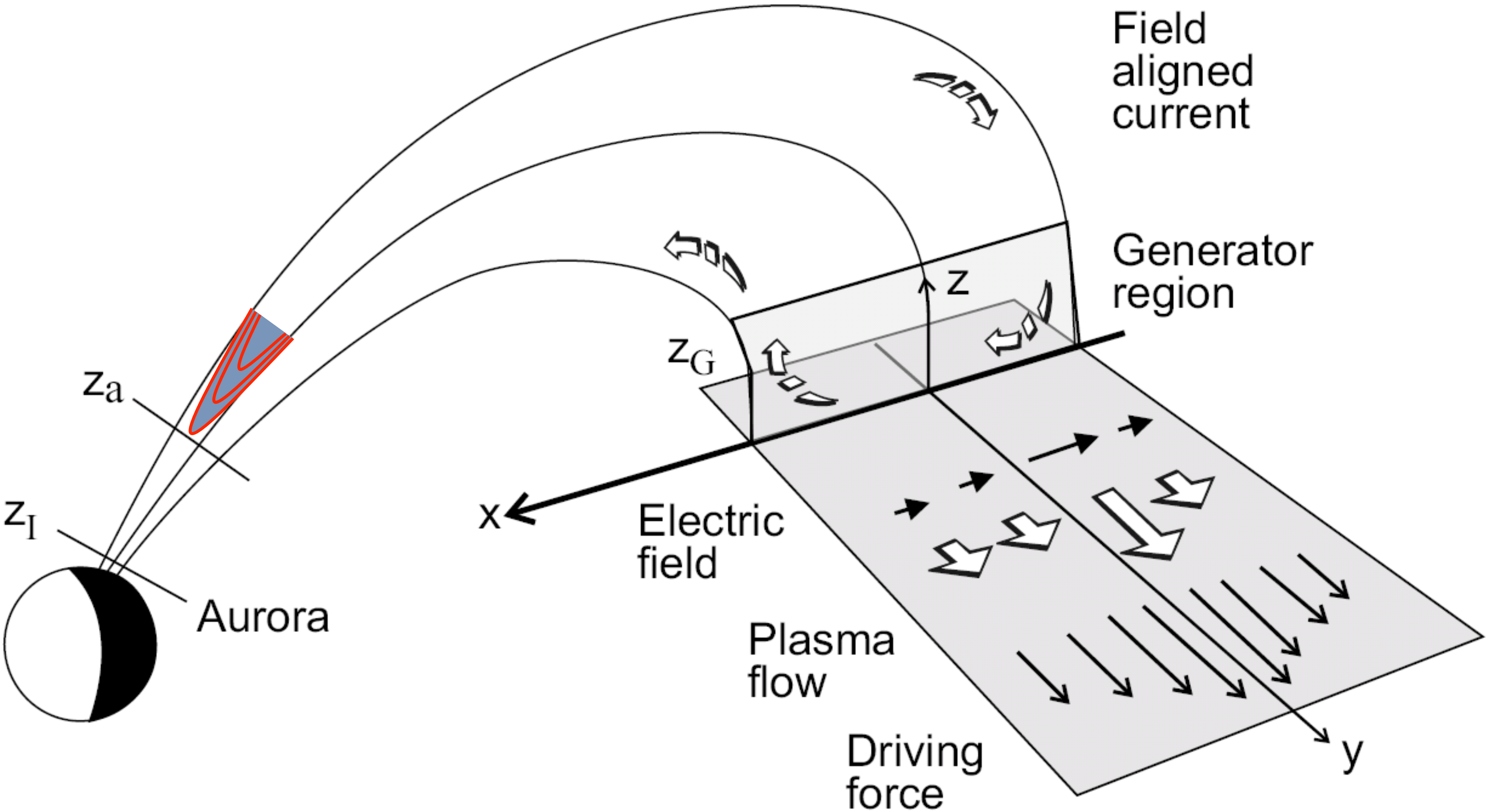


*After Ronmark, JGR 2002*

# Which may be converted to kinetic energy flux of electrons and protons

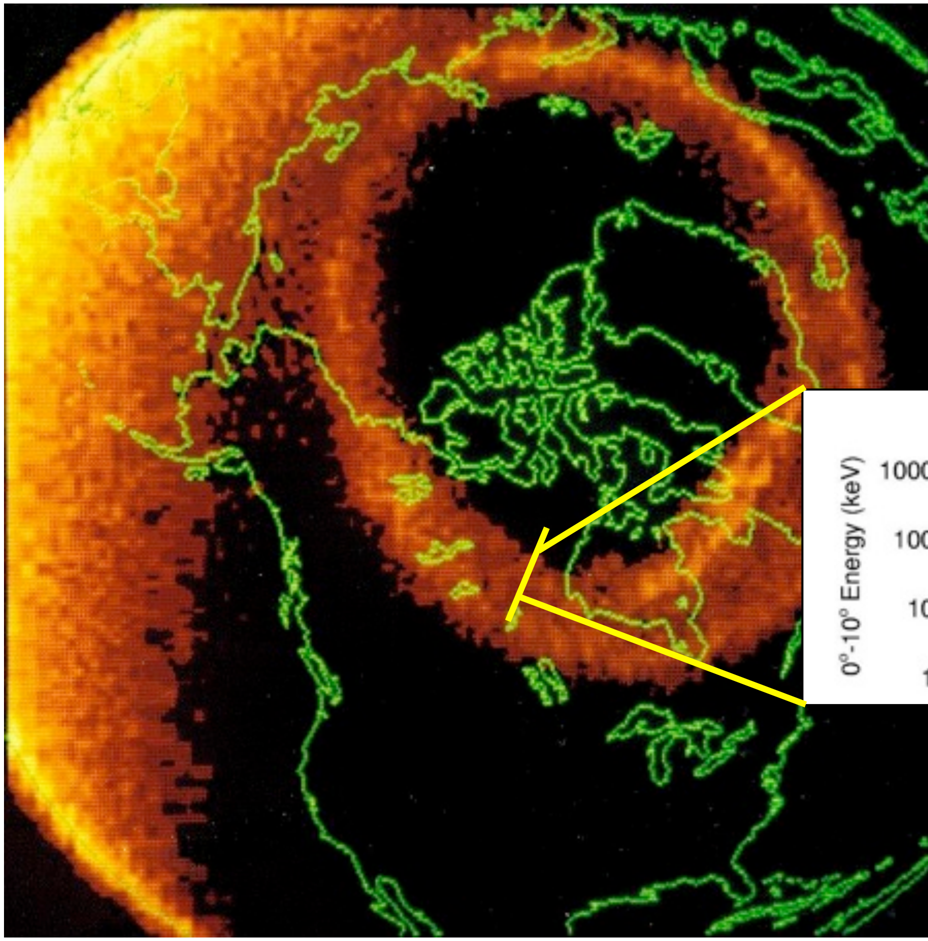

**Kinetic Energy Flux:**

$$\mathbf{K} = \left(\frac{1}{2}\rho u^2\right)\hat{\mathbf{u}}$$

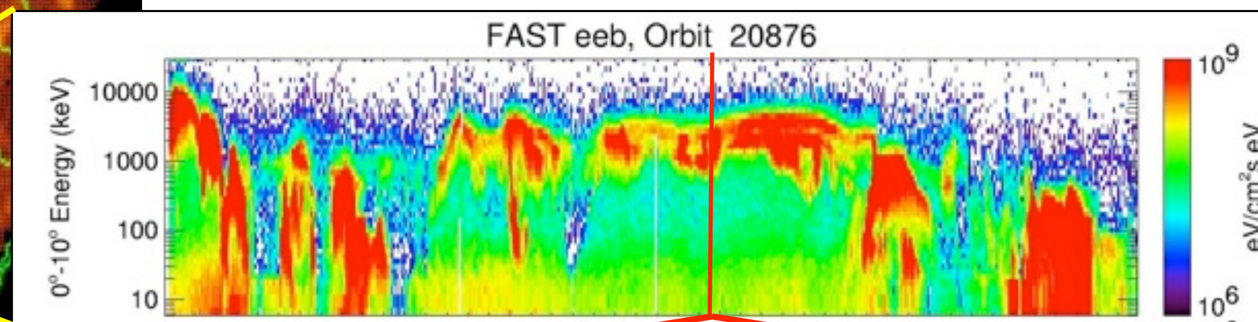


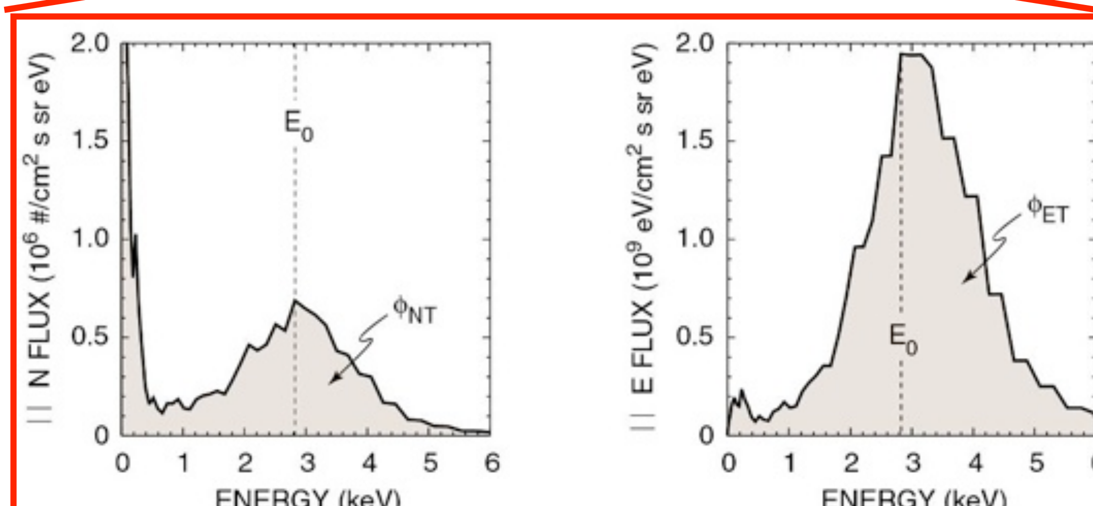


**Some of this electromagnetic energy flux is converted to kinetic energy of electrons and ions in the magnetosphere which, in turn, ionize and excite atmospheric gases to produce the aurora.**

# Imperfect M-I Coupling

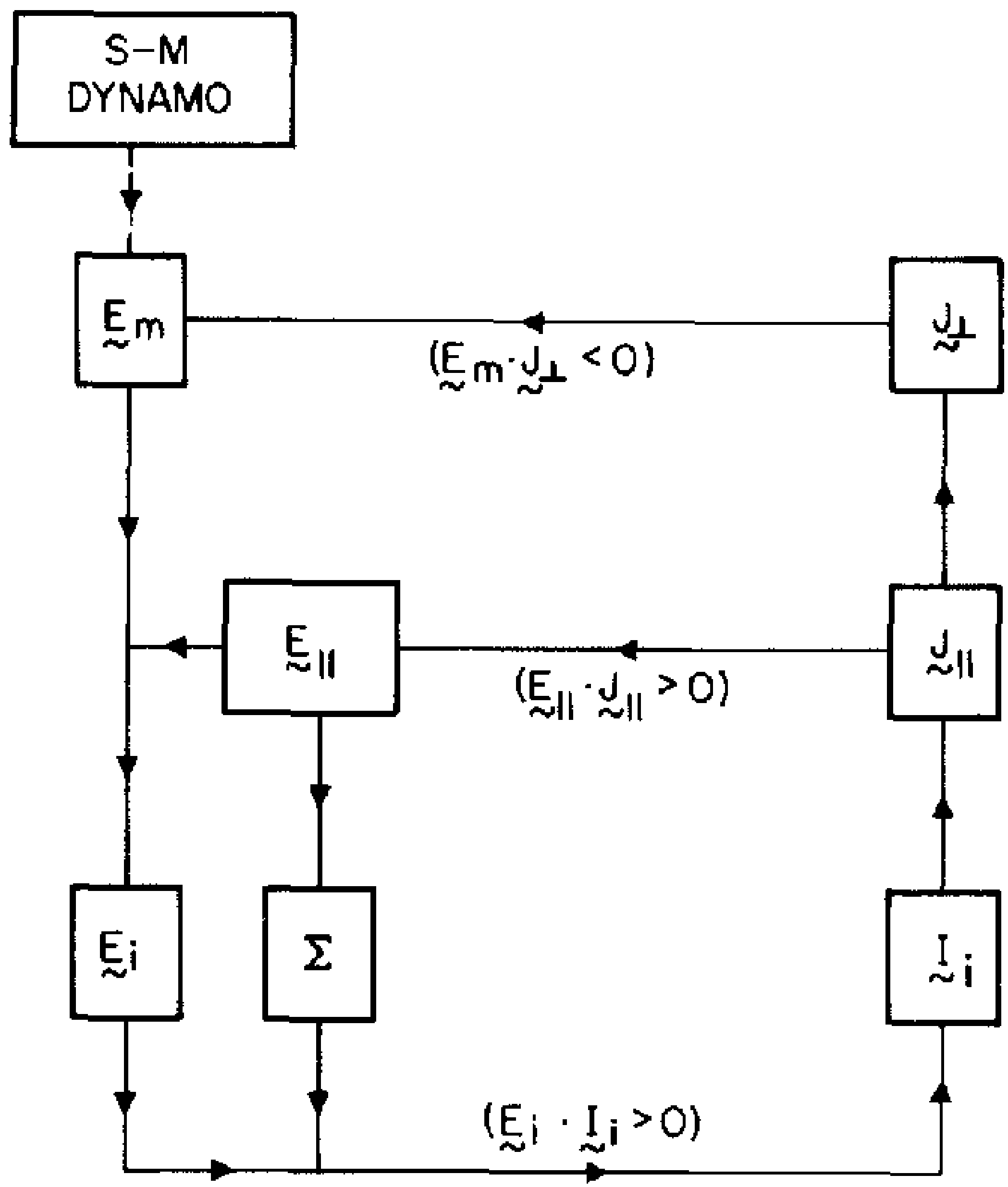


*Kan and Lee, GRL 1980*

# Data manifestations

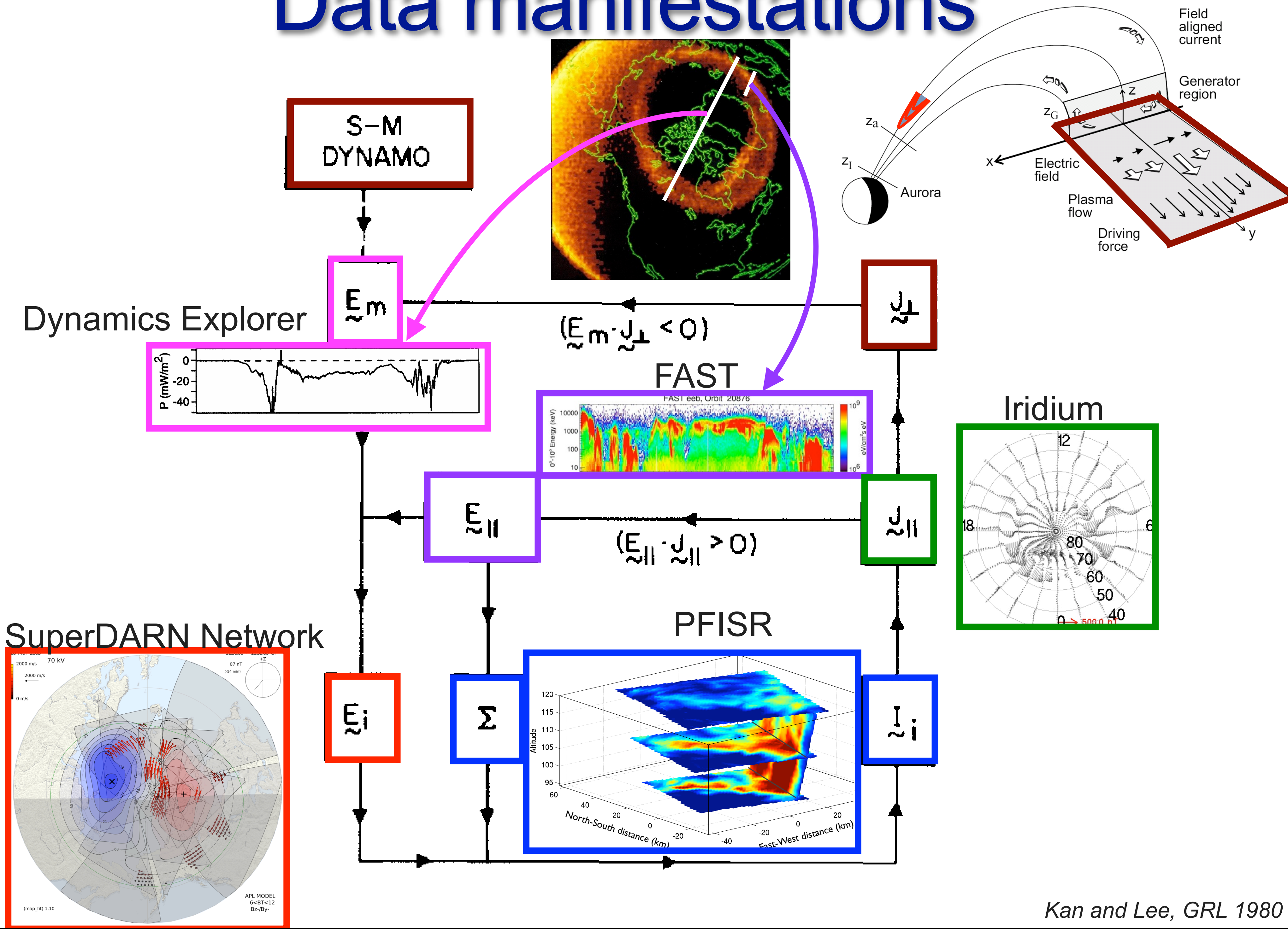


*Kan and Lee, GRL 1980*

# Electron penetration in the ionosphere

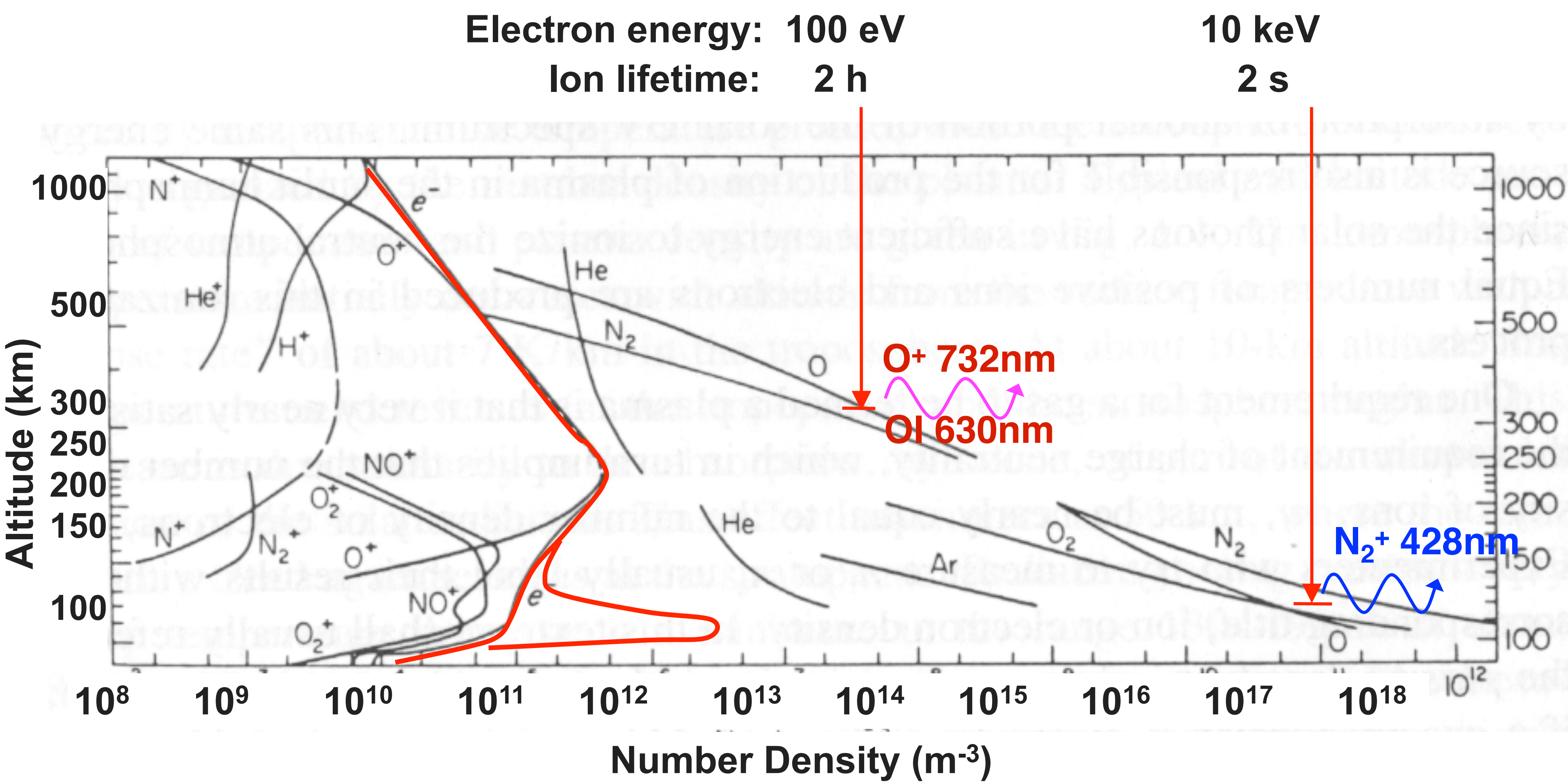


After Kelley, 1989

# Distribution functions and the Boltzmann equation

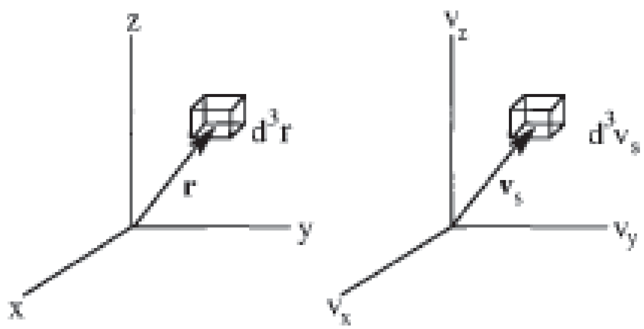


Distribution function $f_s(\boldsymbol{r},\boldsymbol{v}_s,t)$ corresponds to the number of particles of species $s$ that, at time $t$, are located in a volume element $d^3r$ about $\boldsymbol{r}$ have velocities in a velocity-space volume element $d^3v_s$ about $\boldsymbol{v}_s$. Alternatively, $f_s$ can be viewed as a probability density in the $(\boldsymbol{r}, \boldsymbol{v}_s)$ phase space.

$$\frac{\partial f_s}{\partial t} + \boldsymbol{v}_s \cdot \nabla f_s + \boldsymbol{a}_s \cdot \nabla_v f_s = \frac{\delta f_s}{\delta t}$$

Boltzmann equation

$$\frac{\delta f_s}{\delta t} = \iint d^3 v_t \, d\Omega \left| v_s - v_t \right| \sigma_{st}(v_{st},\theta)\left(f_s' f_t' - f_s f_t\right)$$

Boltzmann collision integral

$$\boldsymbol{a}_s = \boldsymbol{G} + \frac{e_s}{m_s}\left(\boldsymbol{E} + \boldsymbol{v}_s \times \boldsymbol{B}\right)$$

Gravitational and Lorentz accelerations

# Electron transport equation

Steady state, no electric field, constant magnetic field

$$\mu \frac{\partial \Phi(E,s,\mu)}{\partial s} = -a - b + c + d + f + Q$$

$$a = \Phi(E,s,\mu) \sum_k n_k(s) \sigma_k^{tot}(E)$$

Losses of electron with energy E and pitch angle $\mu$ due to elastic and inelastic collisions

$$b = n_e(s) \frac{\partial \left( L(E)\Phi \right)}{\partial E}$$

Energy losses due to collisions with thermal electrons

$$c = \sum_k n_k(s) \sigma_k^{el}(E) \int_{-1}^{1} p(E,\mu' \to \mu) \Phi(E,s,\mu') d\mu'$$

Production of electrons with pitch angle $\mu$ due to elastic scattering of electrons with pitch angle $\mu'$

$$d = \sum_k n_k(s) \sum_j \sigma_j^k (E + \Delta E \to E) \int_{-1}^{1} p_j^k (E + \Delta E, \mu' \to \mu) \Phi(E + \Delta E, s, \mu') d\mu'$$

Production of electrons with energy E and pitch angle $\mu$ due to inelastic collisions

$$f = \sum_k n_k(s) \int_{E+\Delta E_{ion}}^{\infty} \sigma_{ion}^k (E' \to E) \int_{-1}^{1} p_{ion}^k (E', \mu' \to \mu) \Phi(E', s, \mu') dE' d\mu'$$

Production of secondary electrons with energy E and pitch angle $\mu$ in ionization

# Characteristic State Response

Mono-energetic beams with $\int E f(E) dE = 1 \text{ mW/m}^2$

100eV = 250 km    1keV = 150 km

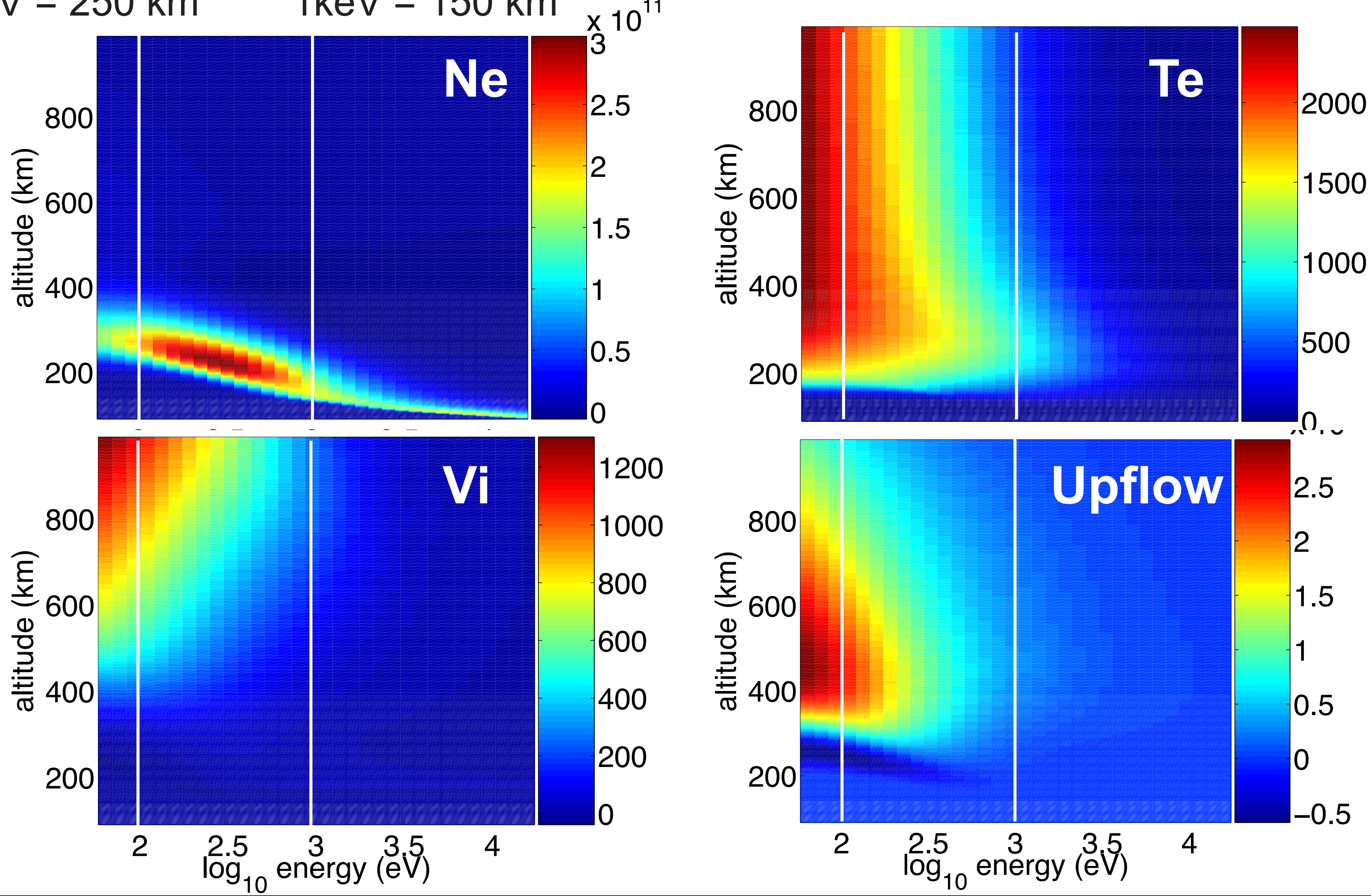

# Step Response:  26 March 2008

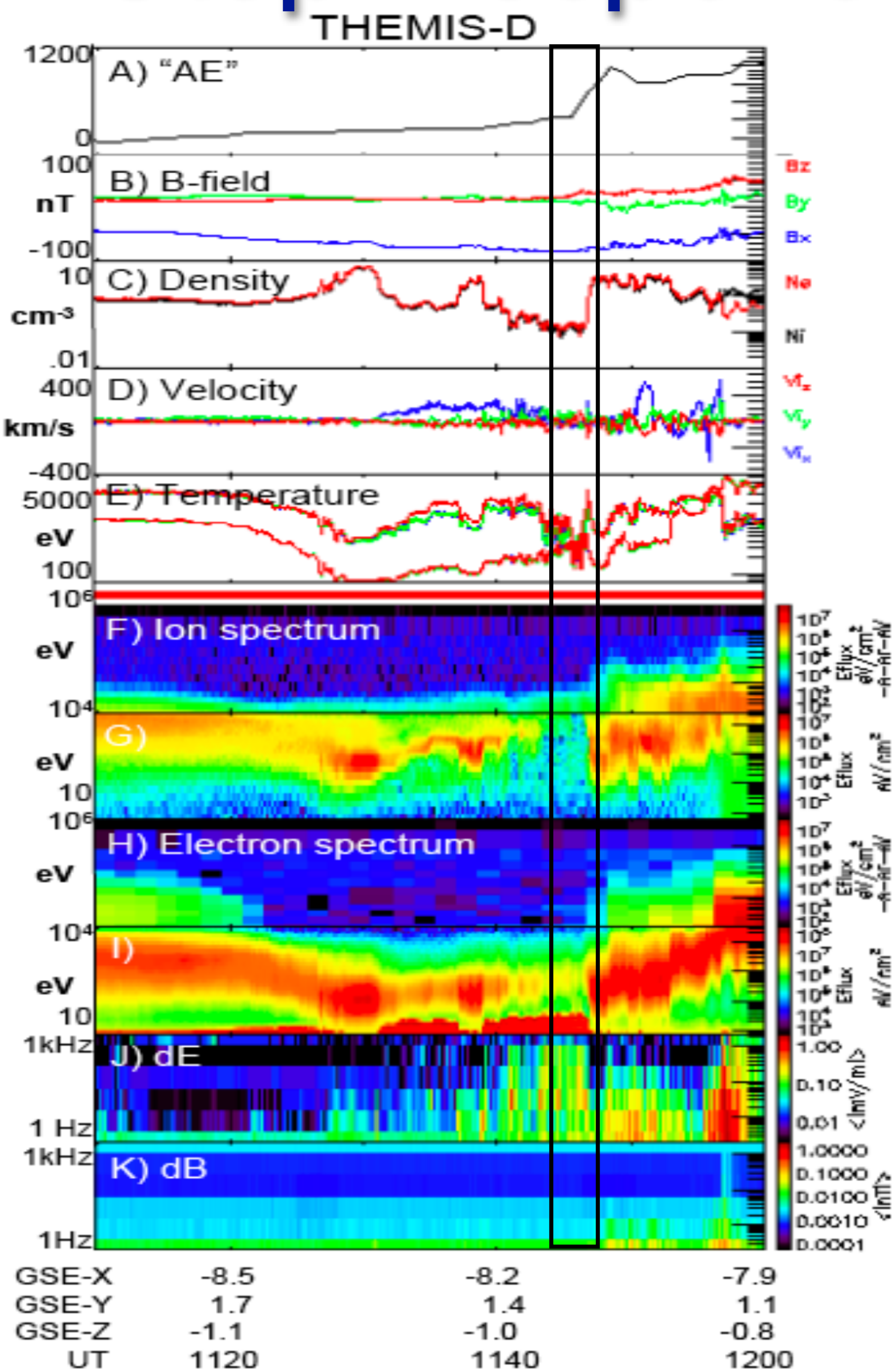


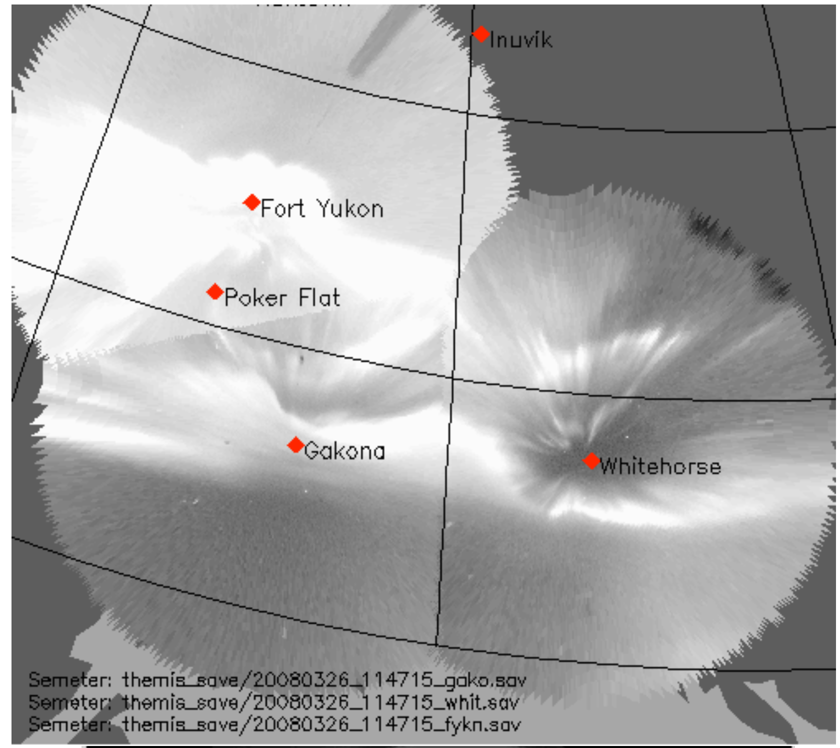


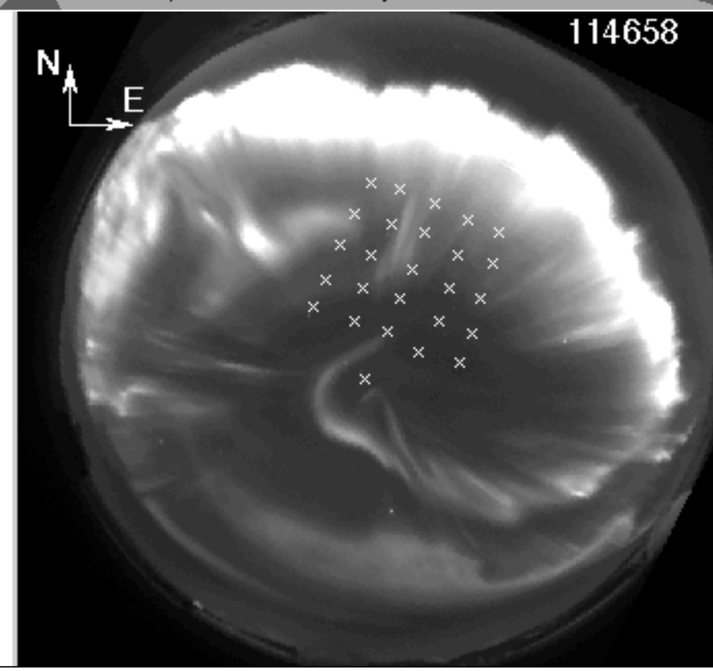

# Ionospheric forensics

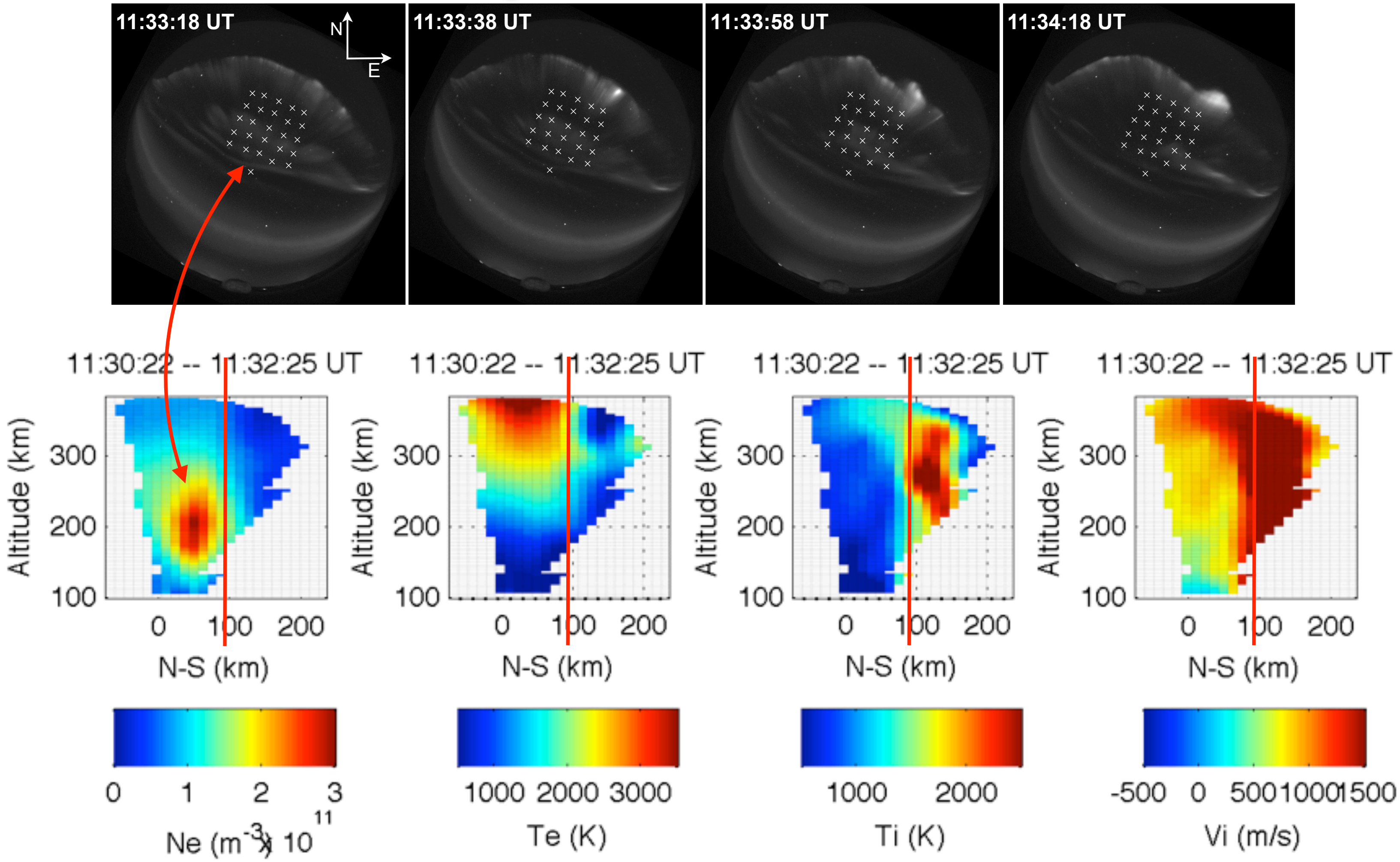


300 eV primaries

Ion frictional heating, strong E-field at poleward boundary

Mixture of convective flow and field-aligned upflow at boundary.

*Semeter et al., JGR 2012, in press*

# Composite imaging

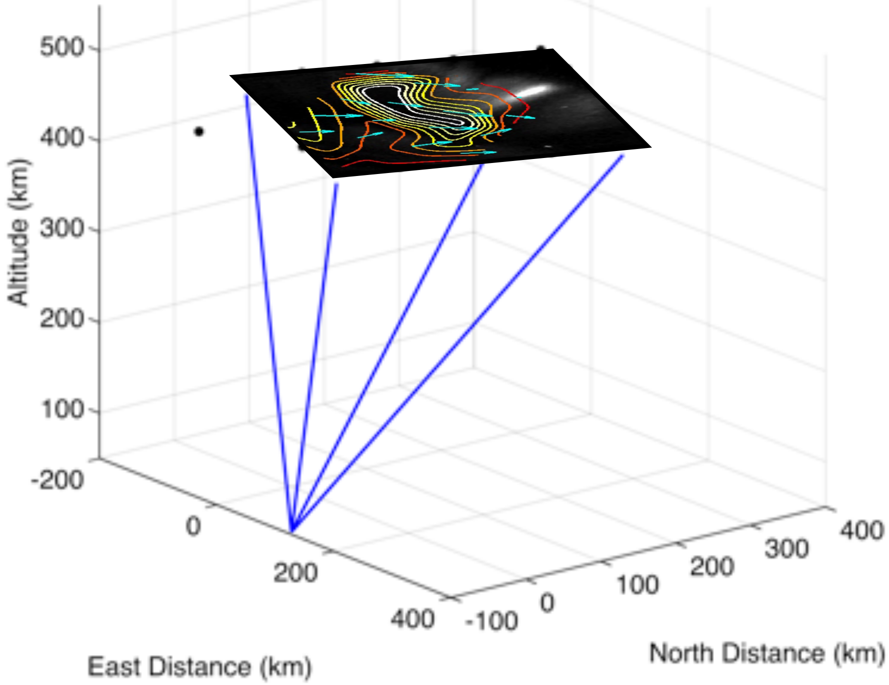


$$v_{los} = \mathbf{k} \cdot \begin{bmatrix} v_e & v_n & v_{\|} \end{bmatrix}^T$$

$$\mathbf{k} = \begin{bmatrix} \cos\theta\sin\phi \\ \cos\theta\cos\phi \\ \sin\theta \end{bmatrix}^T \begin{bmatrix} \cos\delta & \sin I\sin\delta & -\cos I\sin\delta \\ -\sin\delta & \cos\delta\sin I & -\cos I\cos\delta \\ 0 & \cos I & \sin I \end{bmatrix}$$

$$\begin{bmatrix} v_{los}^1 \\ v_{los}^2 \\ \vdots \\ v_{los}^i \\ \vdots \\ v_{los}^N \end{bmatrix} = \begin{bmatrix} \mathbf{k}^1 \\ \mathbf{k}^2 \\ \vdots \\ \mathbf{k}^i \\ \vdots \\ \mathbf{k}^N \end{bmatrix} \mathbf{v} + \begin{bmatrix} e_{los}^1 \\ e_{los}^2 \\ \vdots \\ e_{los}^i \\ \vdots \\ e_{los}^N, \end{bmatrix}$$

$$\mathbf{v}_{los} = A\mathbf{v} + \mathbf{e}_{los}$$

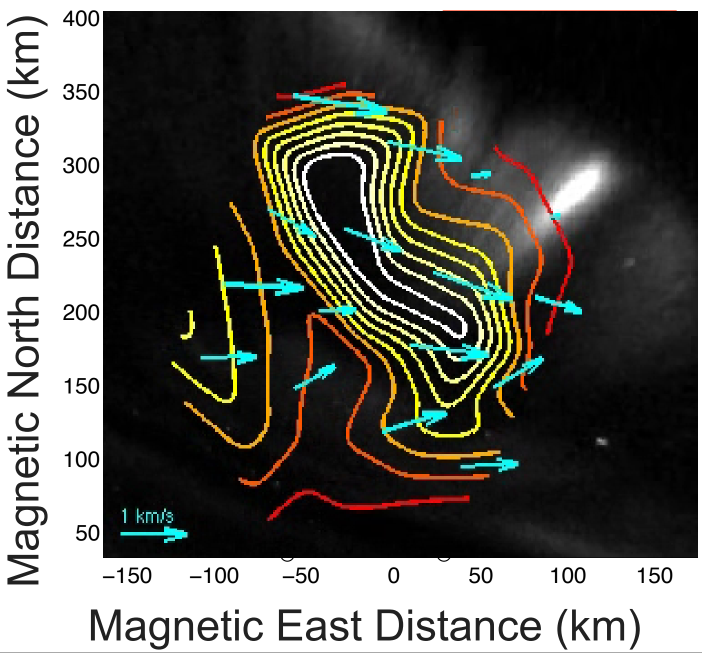

# Ionospheric forensics

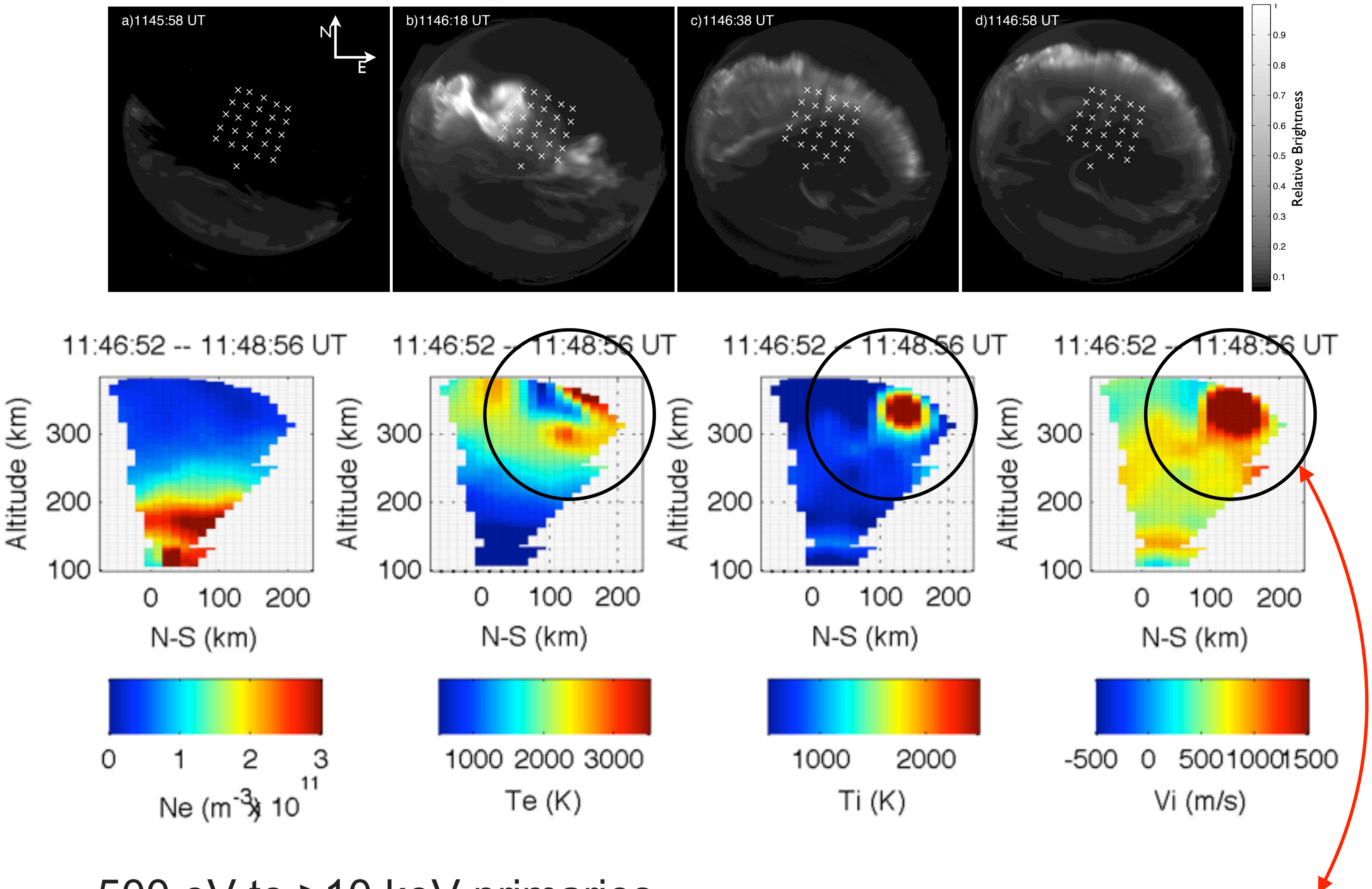


500 eV to >10 keV primaries

Something strange in the ion-acoustic spectrum

Semeter et al., JGR 2012, in review

# 3D Imaging of substorm ionization: 10 Nov 2007

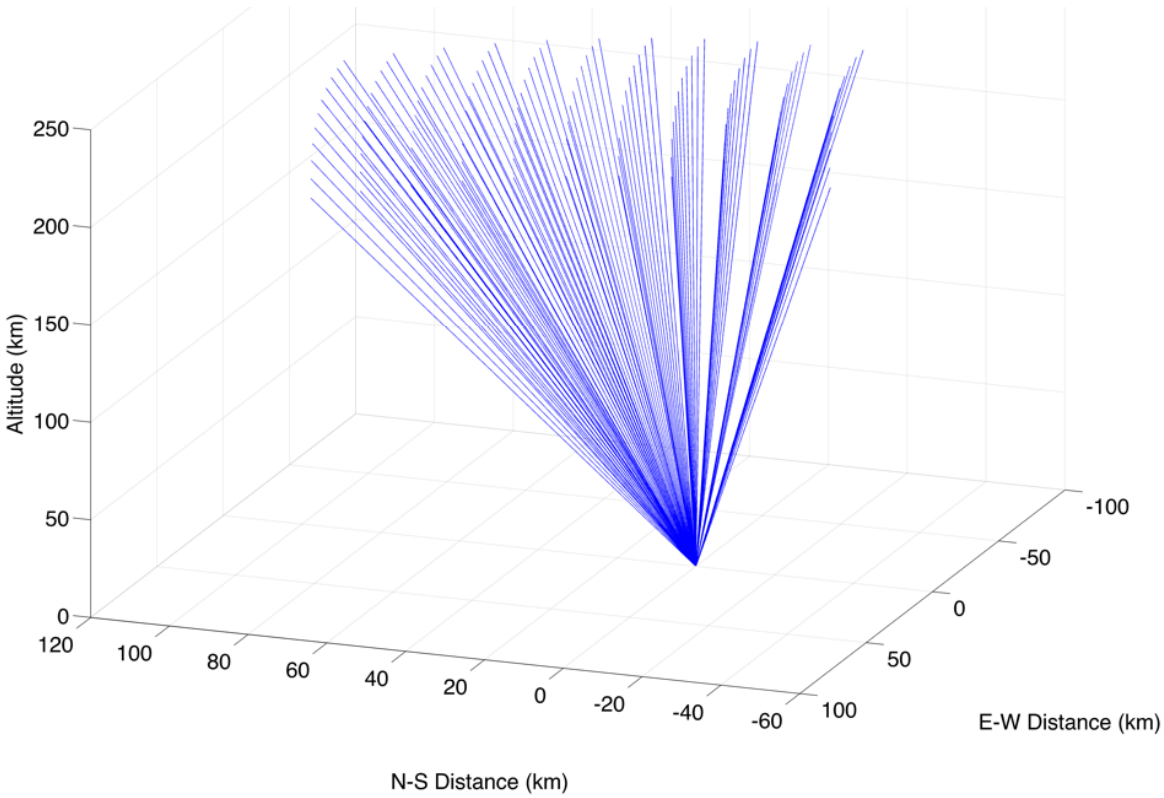


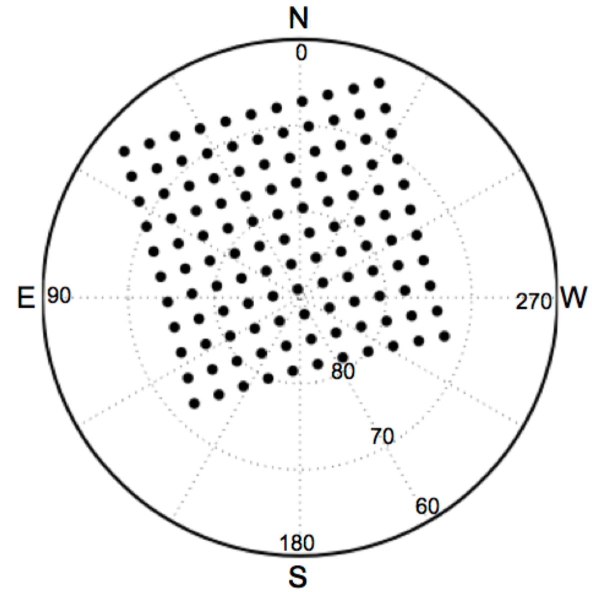


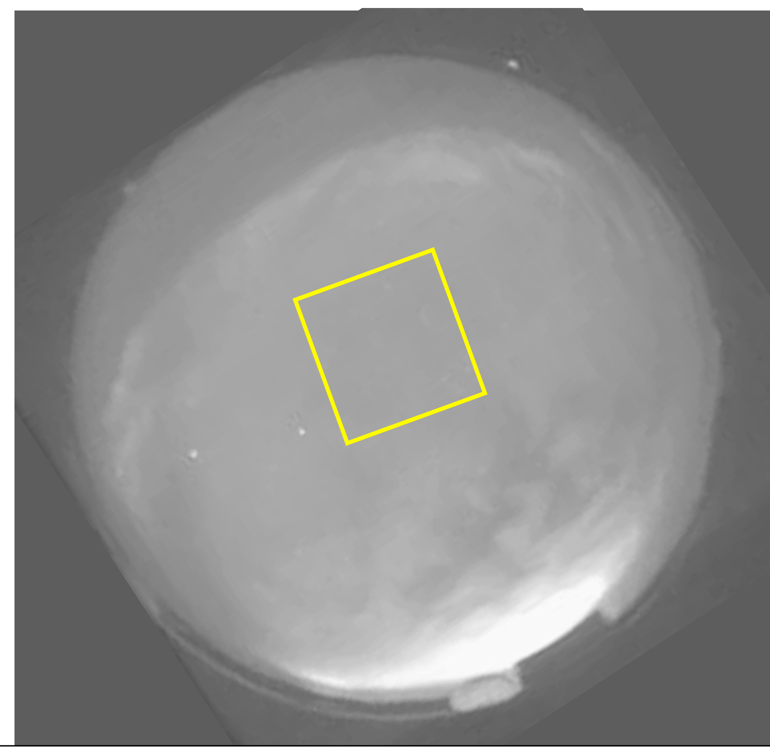

11x11 grid of beams
3 deg separation
Two pulse patterns:
- 13 Baud Barker code
- 480us uncoded pulse

14.6 s integration = 48 pulses/beam

# Volumetric view

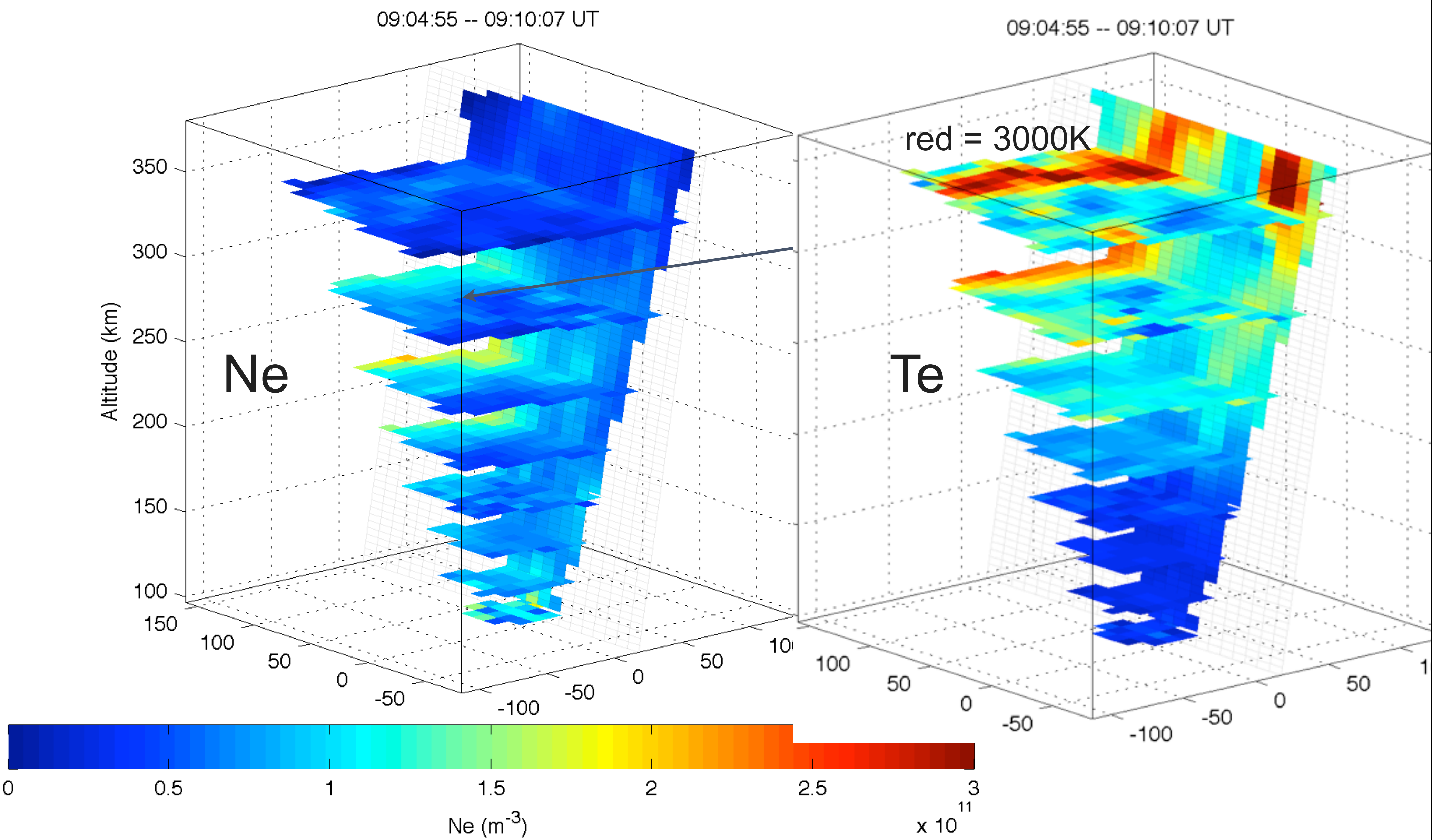

# Volumetric view

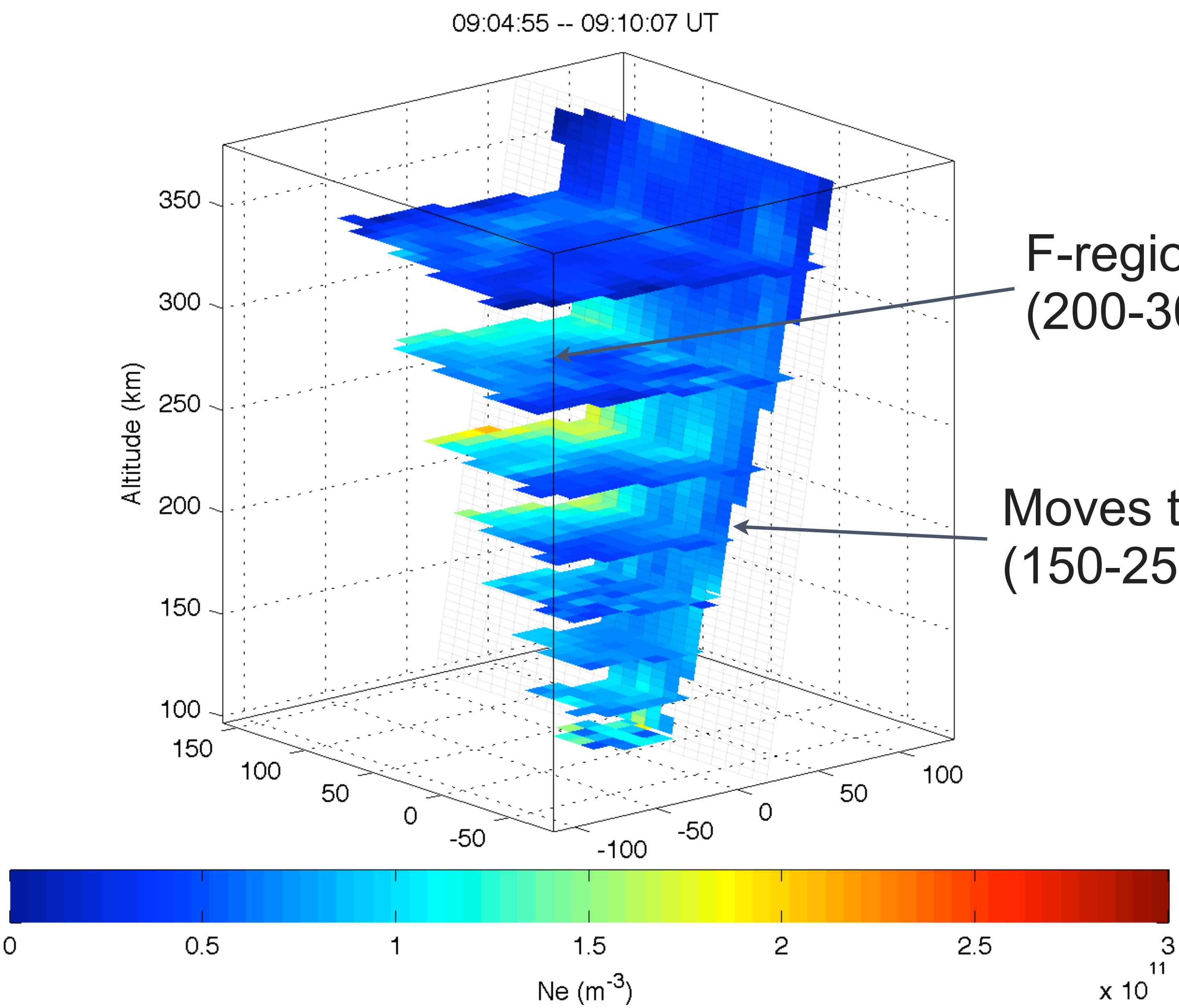


F-region production
(200-300 km, t-20min)

Moves to lower altitude
(150-250km, t-5min)

# Volumetric view

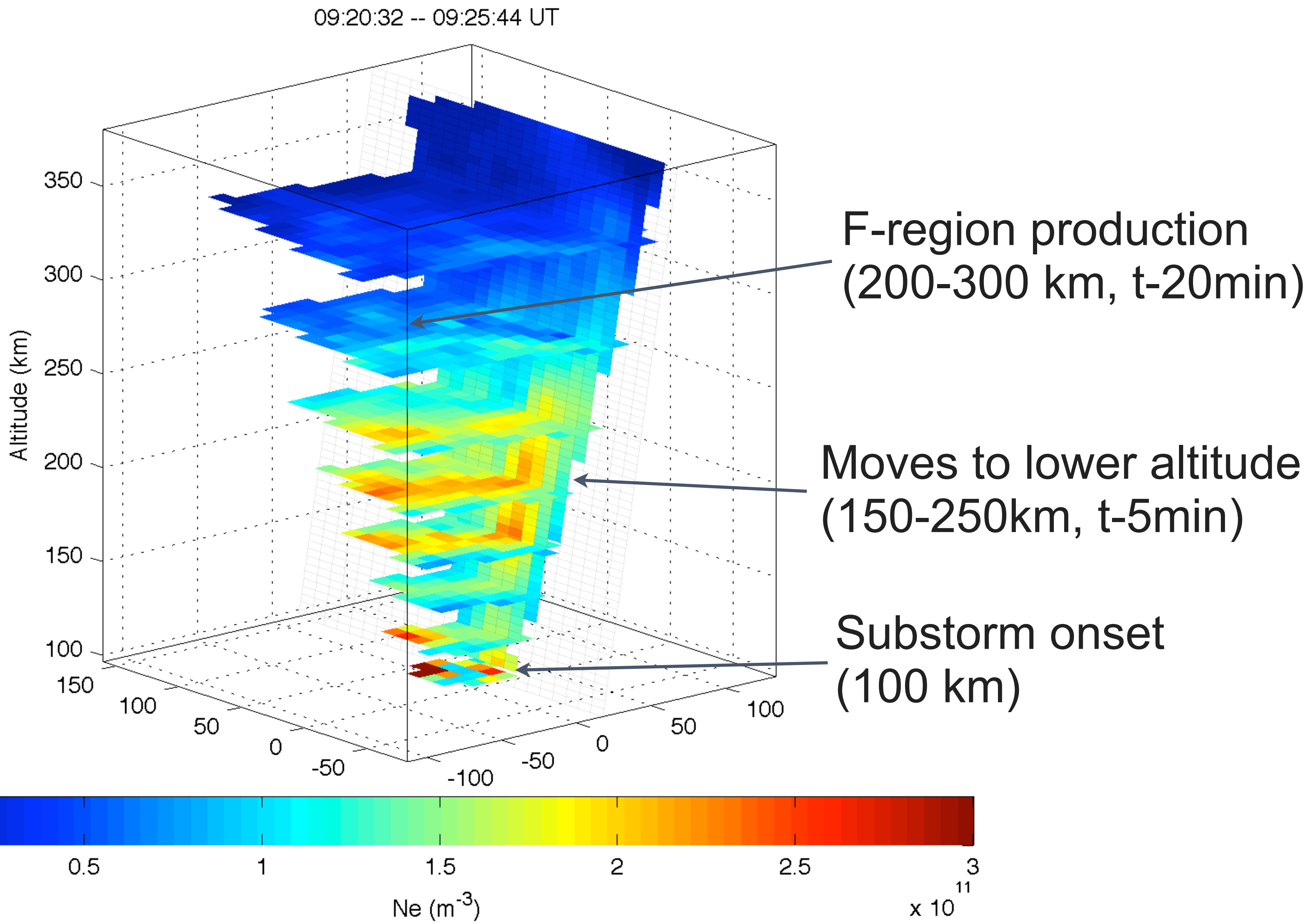

# Volumetric view

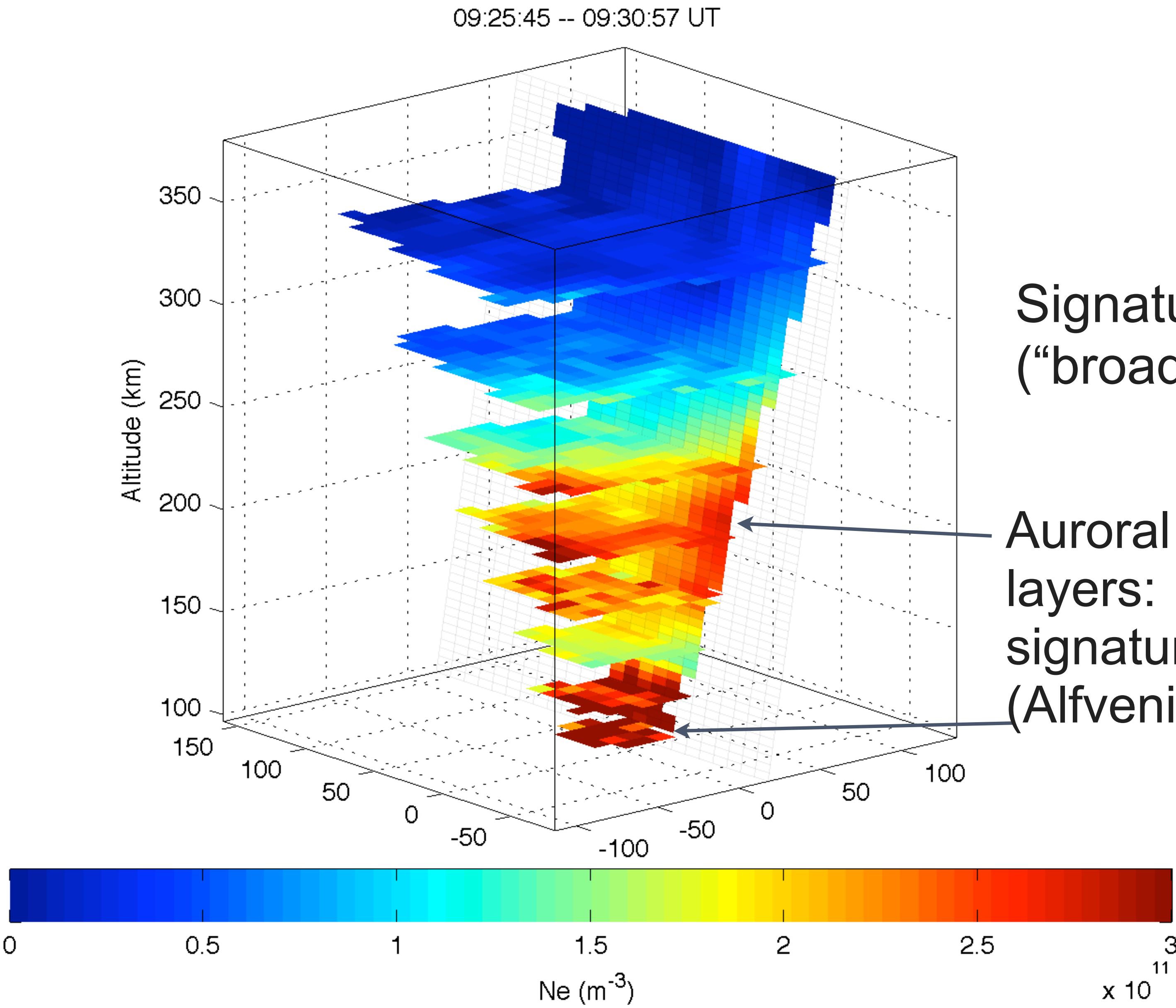


Signature of Alfvenic ("broad band") precipitation

Auroral ionization in two layers:
signature of broad (Alfvenic) energy distribution

# “Growth phase” arcs

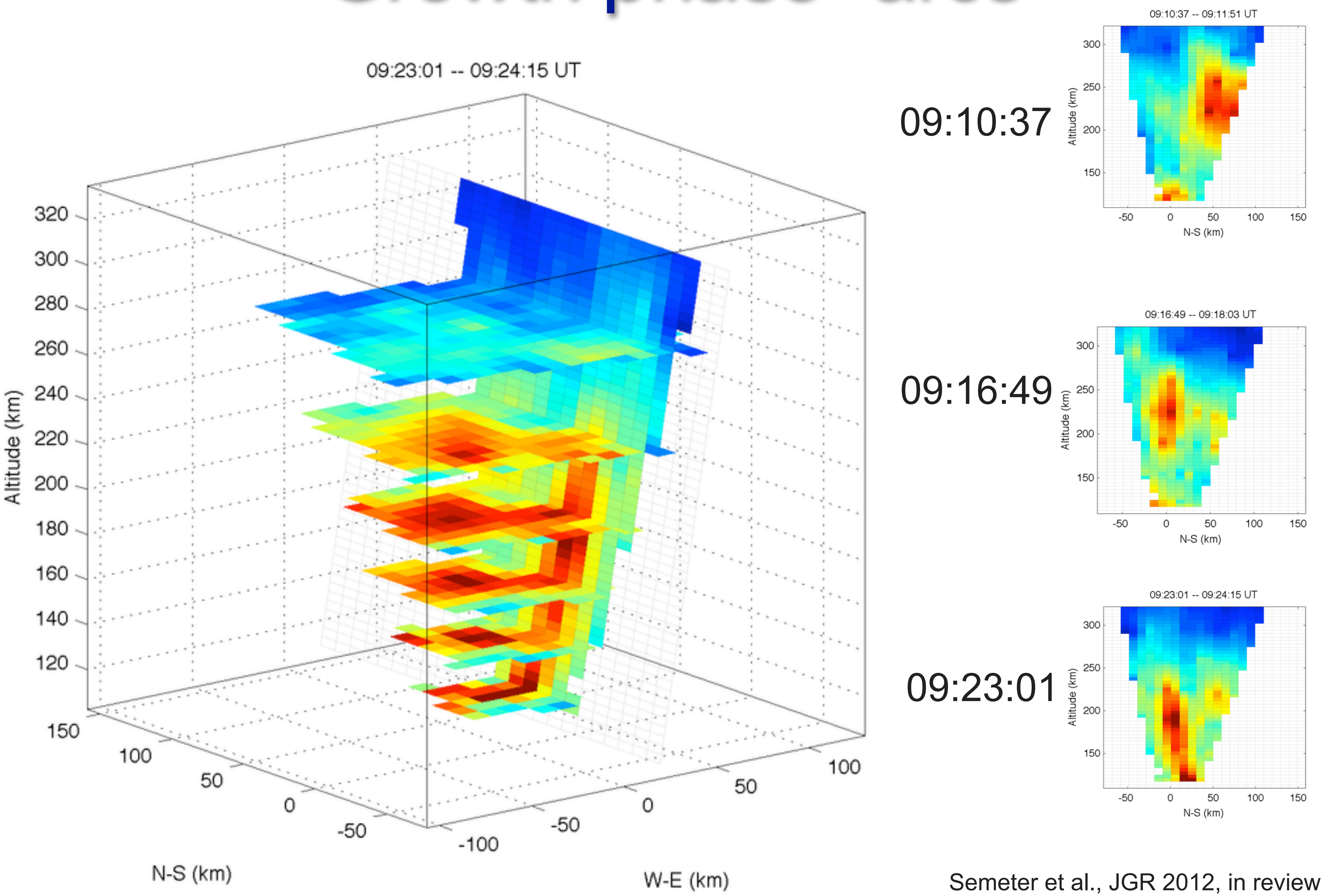


Semeter et al., JGR 2012, in review

# Barker Code (15-s integration)

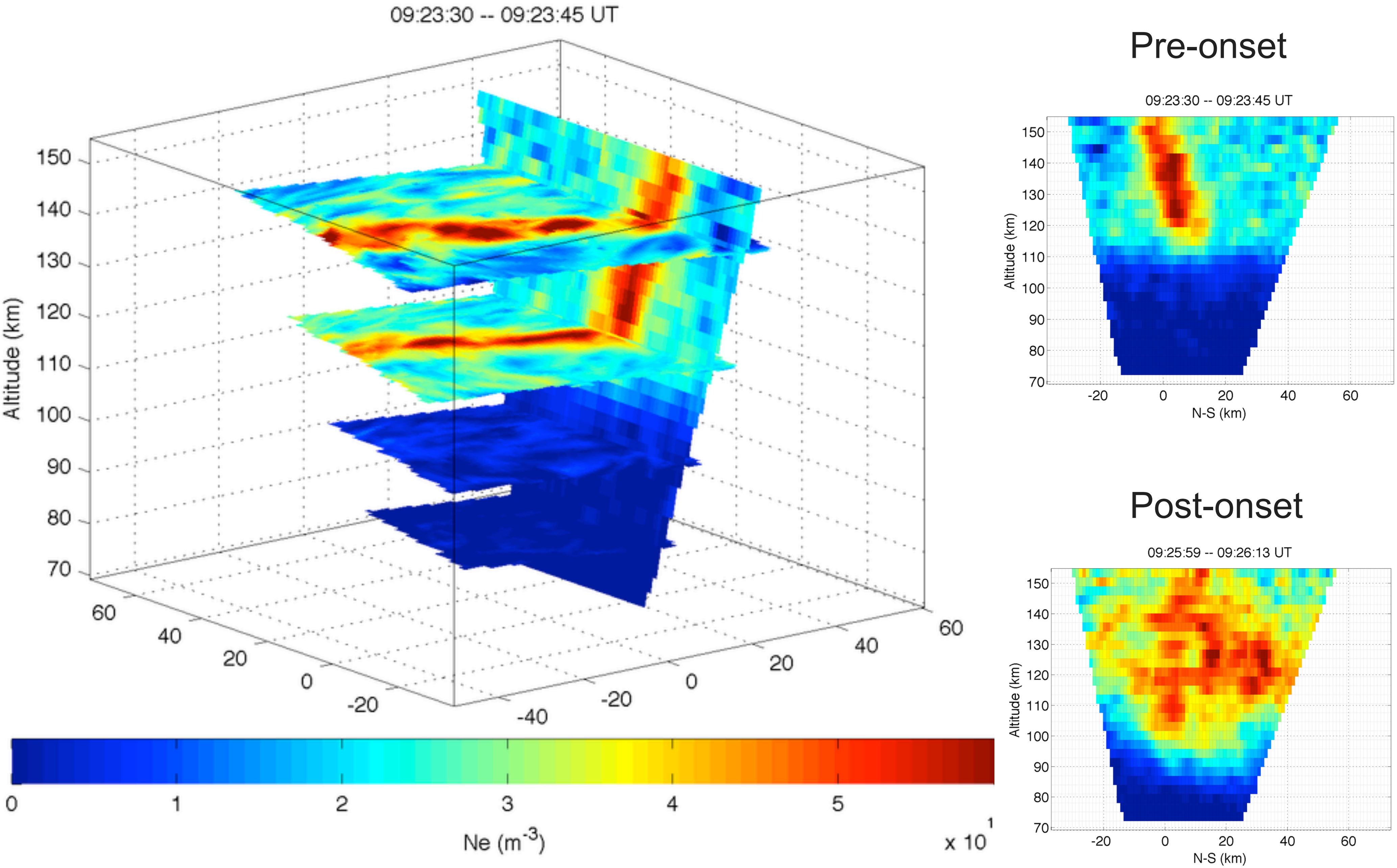

# PFISR non-thermal echoes at onset

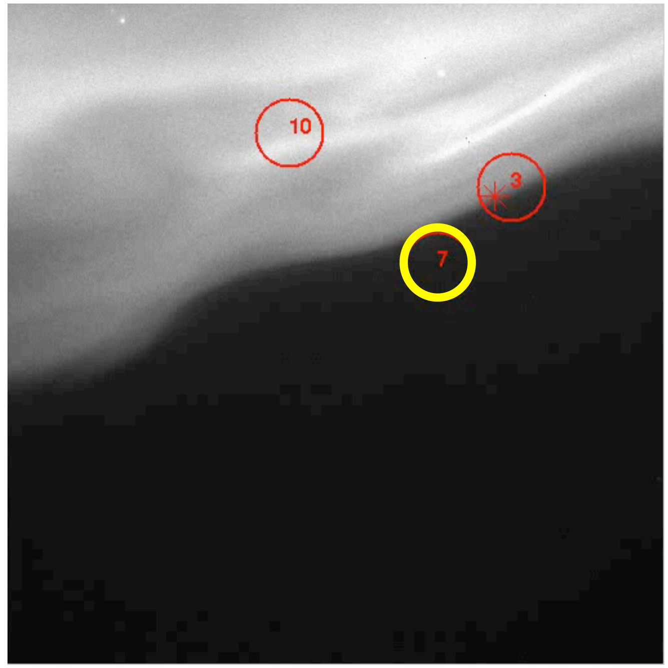


11° x 11°
field-of view

21 x 21 km

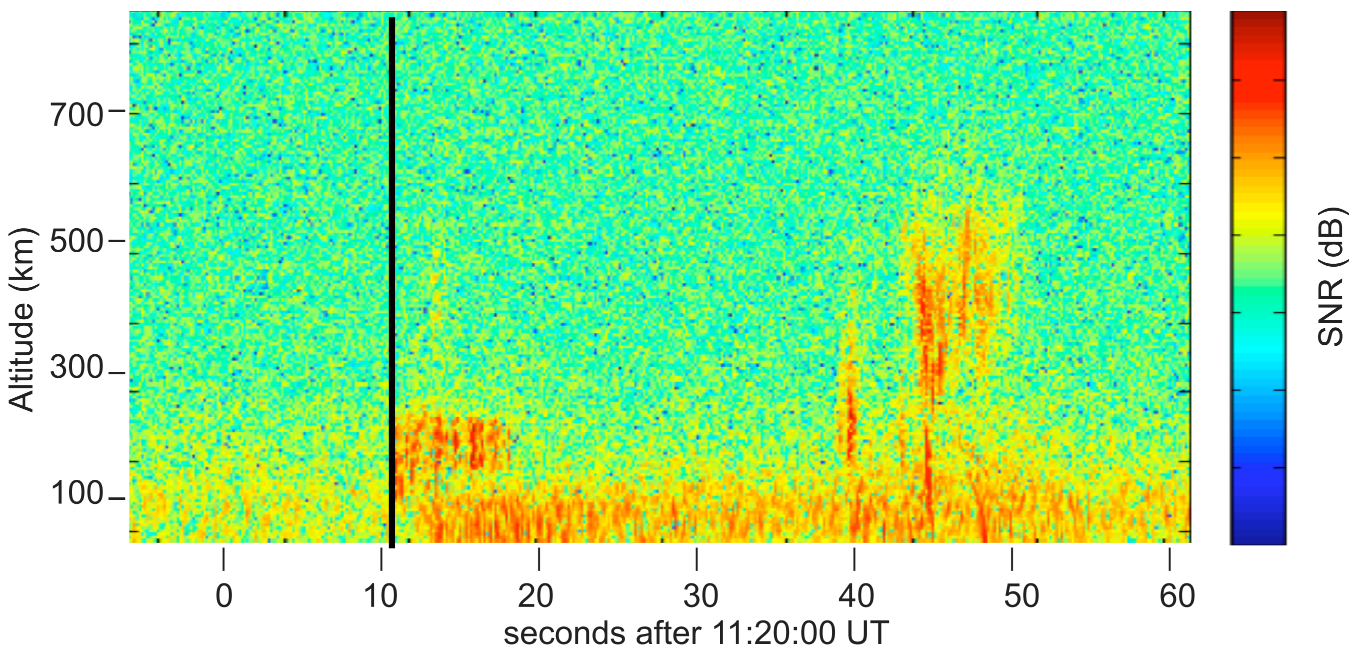


Semeter et al., JGR 2009, Akbari et al., GRL 2012

# Non-thermal PFISR echoes

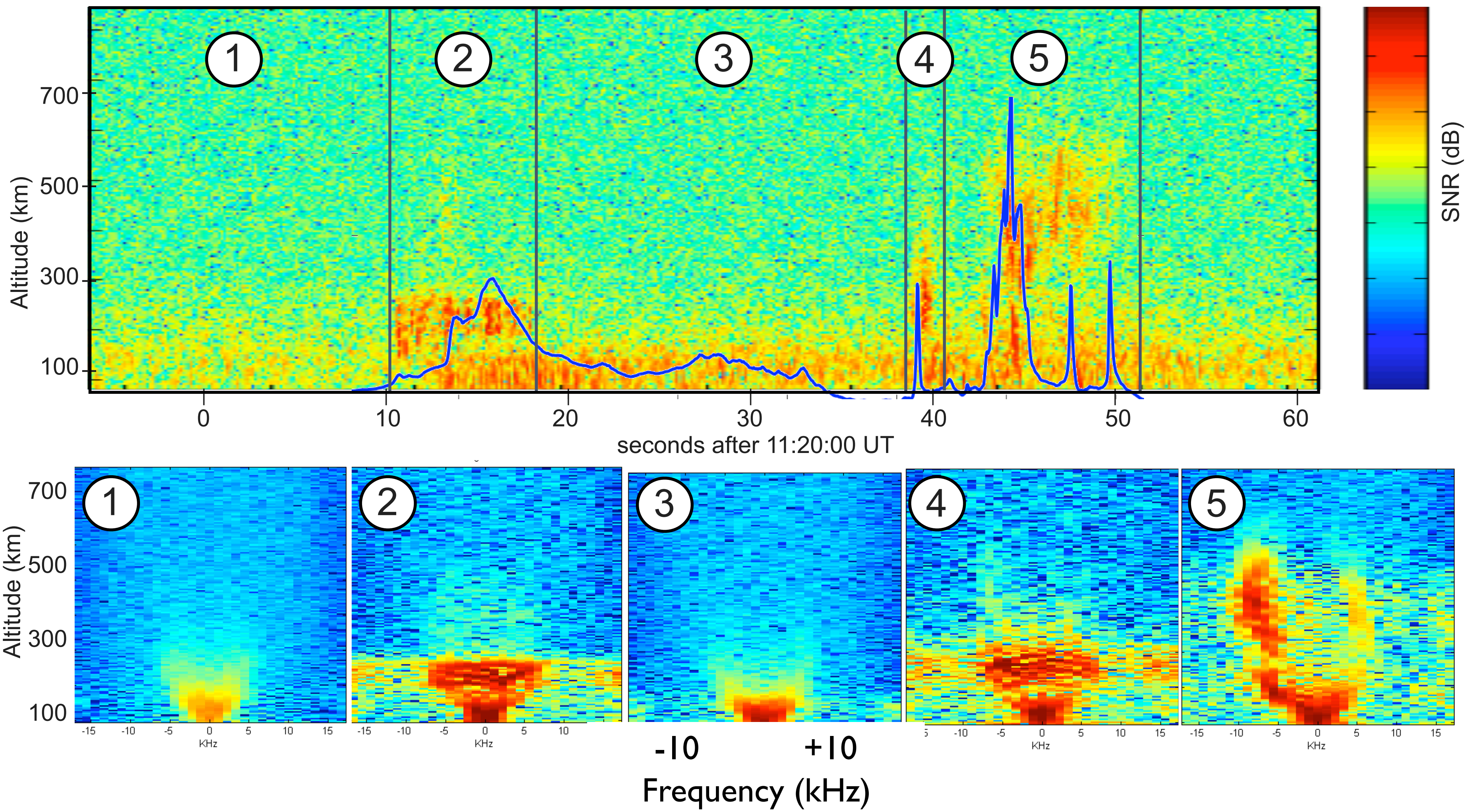


Akbari et al., GRL 2012

# Beam destabilized plasma

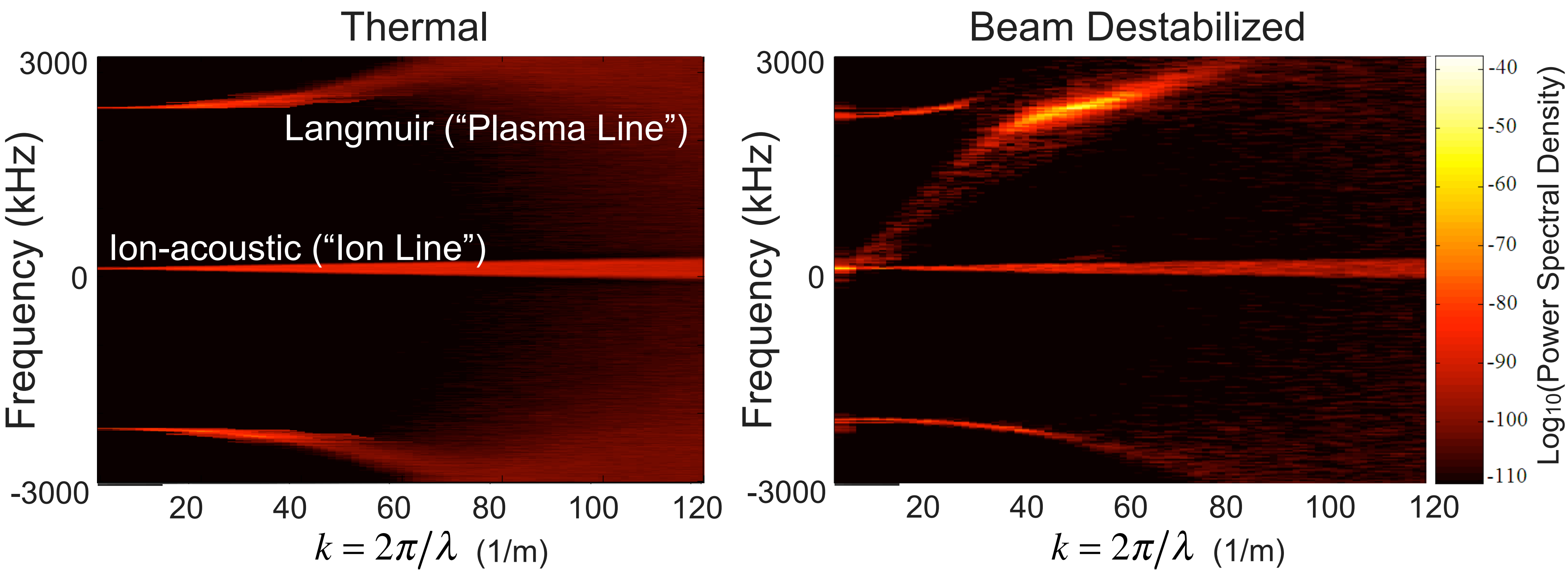


Parametric decay of Langmuir waves produces enhancement in ion-acoustic waves

Diaz et al., JGRA 2011

# Technical challenge: Perspective and Photometry

Oxygen ion production above 300 km, requires intense flux of low-energy (<100 eV) electrons.

Evidence for wave acceleration of ambient ionospheric ions.

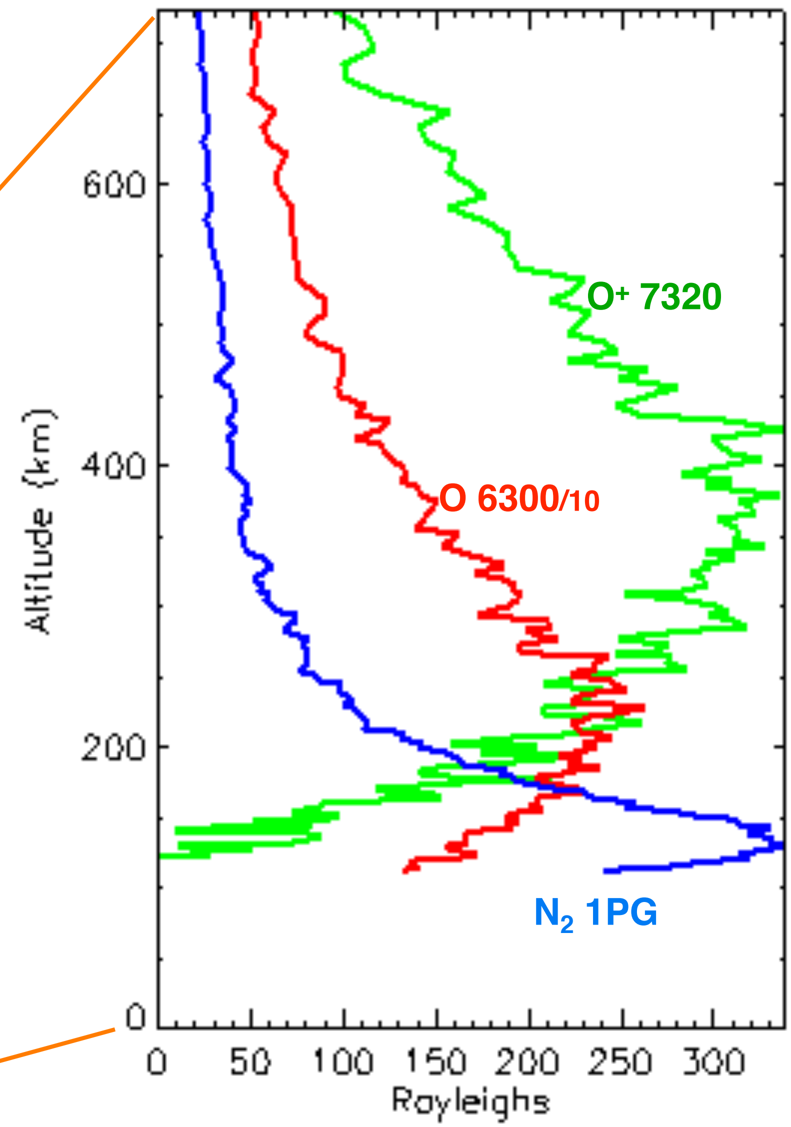


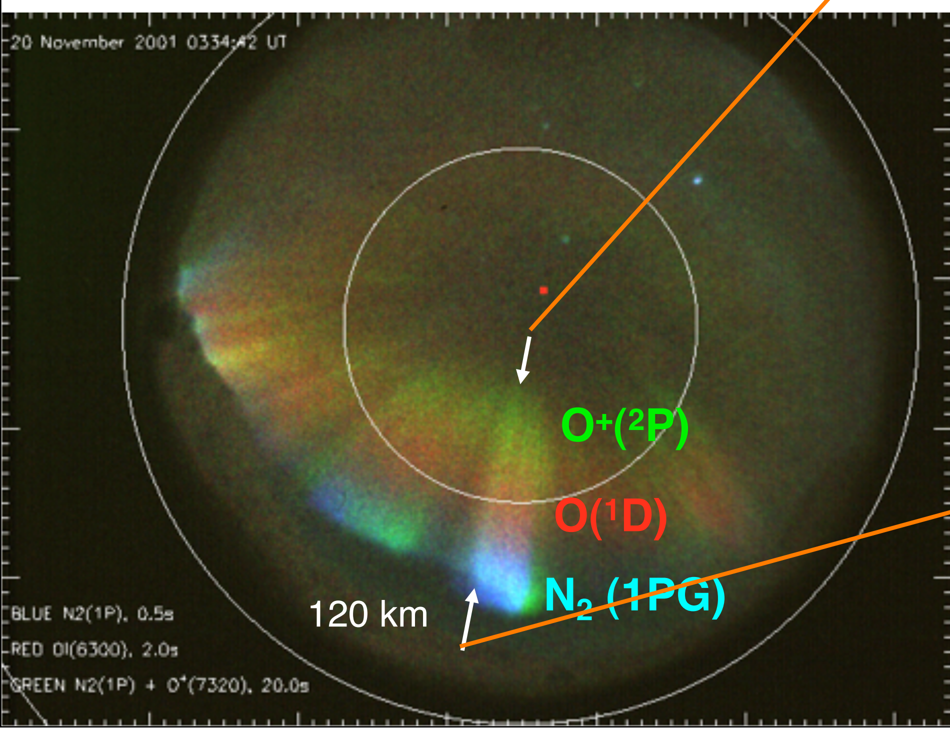


Semeter, GRL 2003

# What does the aurora do to the ionosphere?

Result is column of ionization, 1 X 200 km.
Presents highly structured conductivity.
Provides additional source for ion extraction.

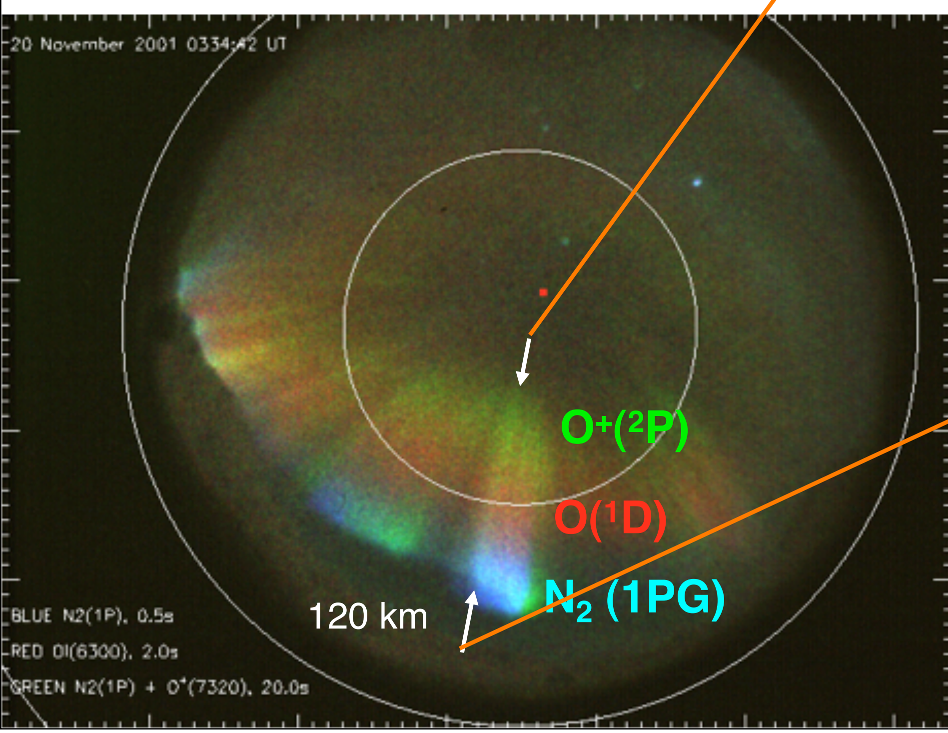


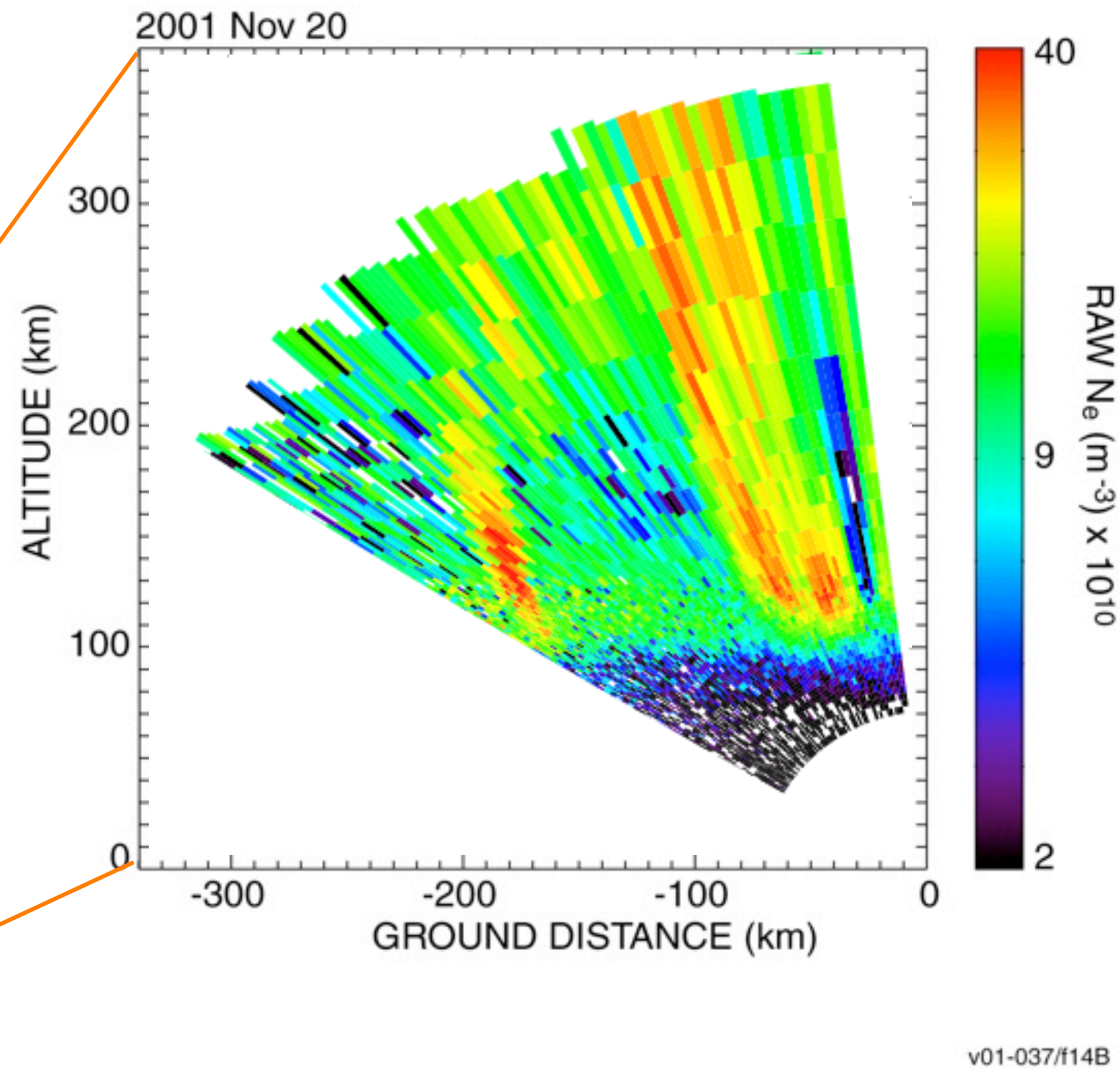


Semeter et al., JGRA 2005

# Forward modeling of optical and radar parameters

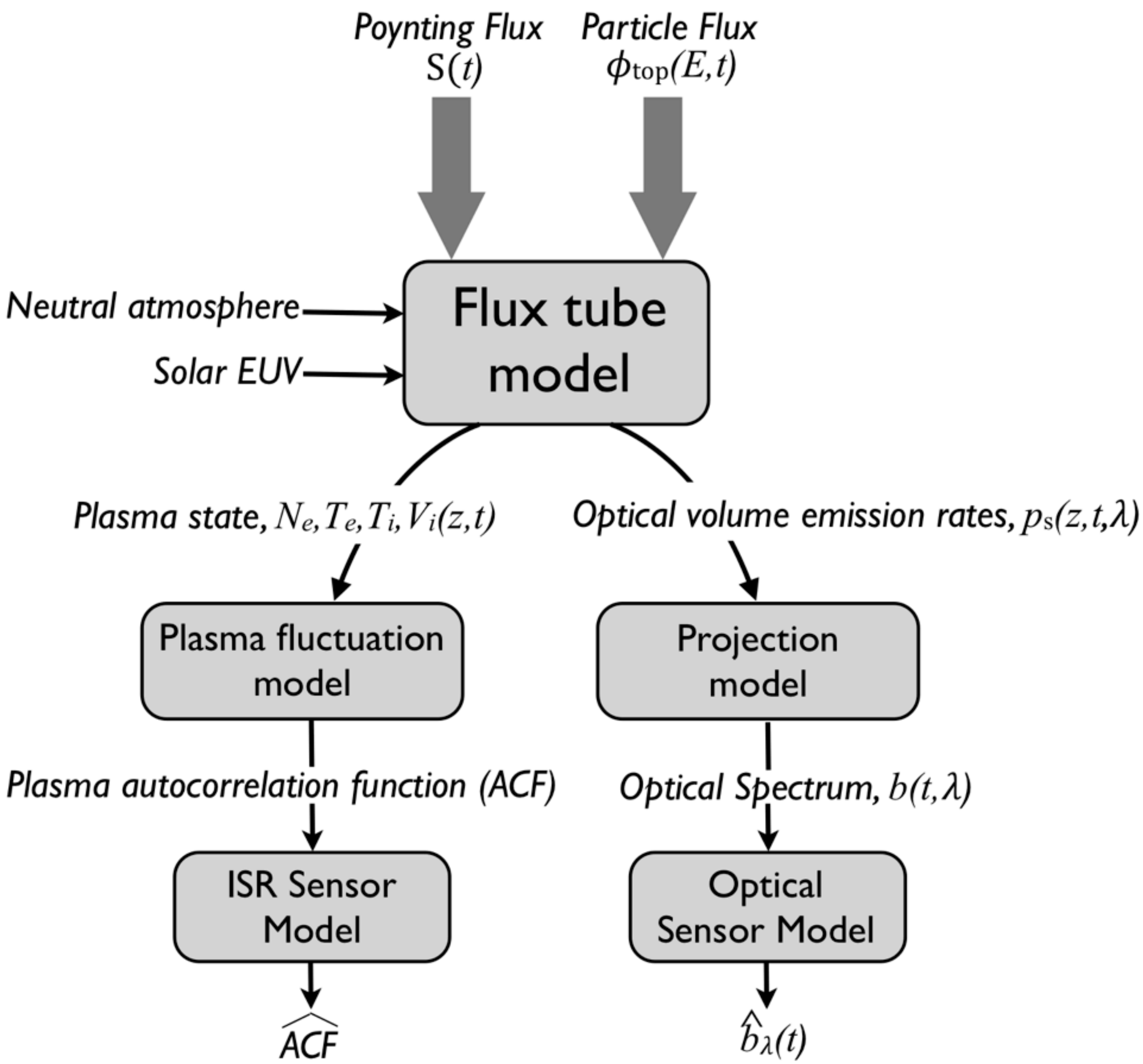

# PFISR Low Duty Cycle Operations: Corotating Interaction Regions

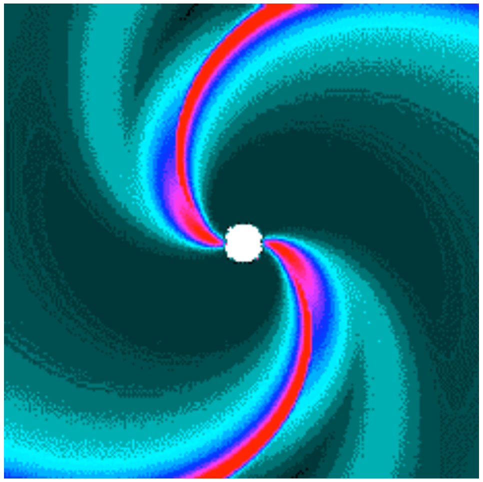

Corotating Interaction Region

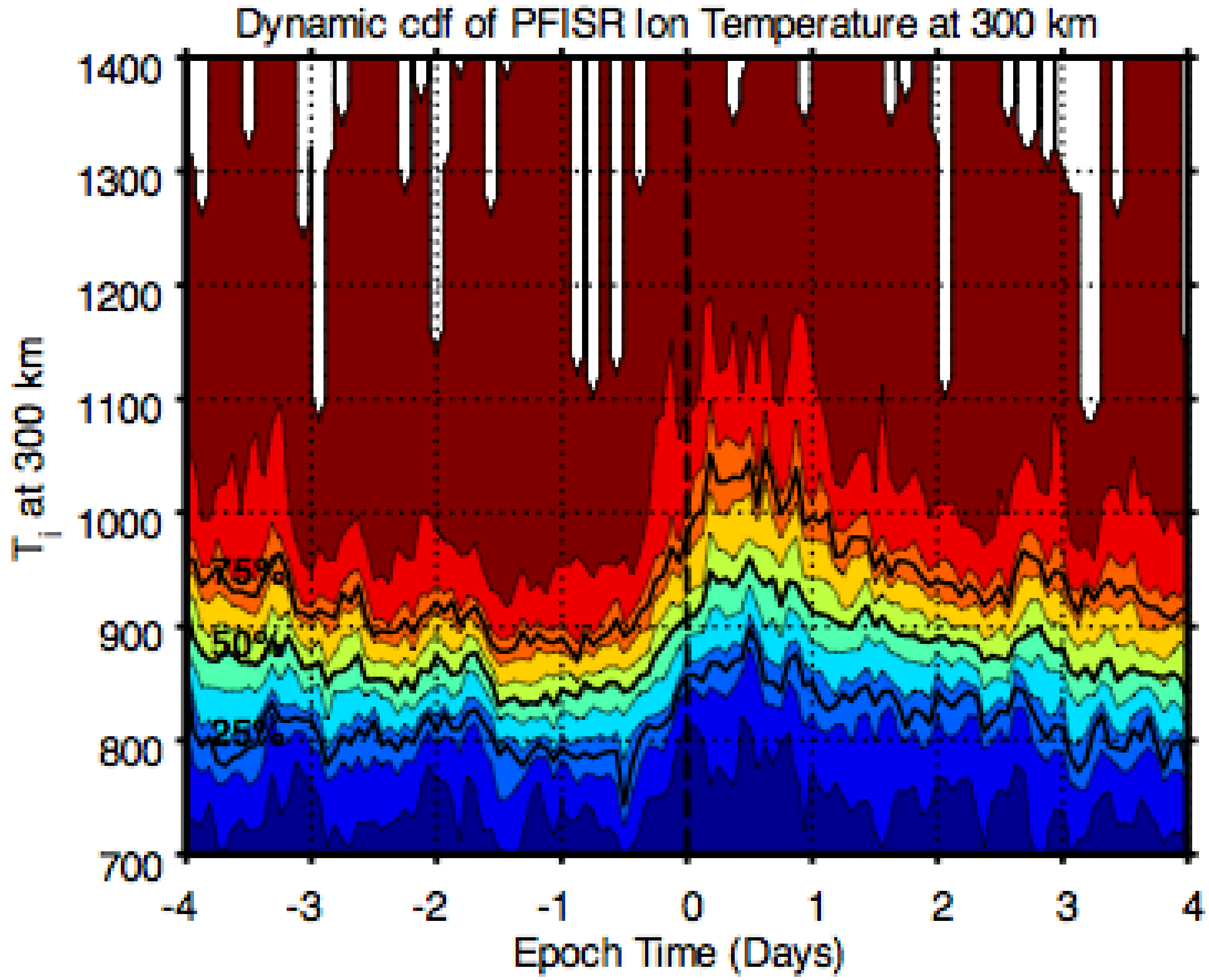


Sojka et al., GRL 2009.

# PFISR Low Duty Cycle Operations: Solar wind - Ti coupling

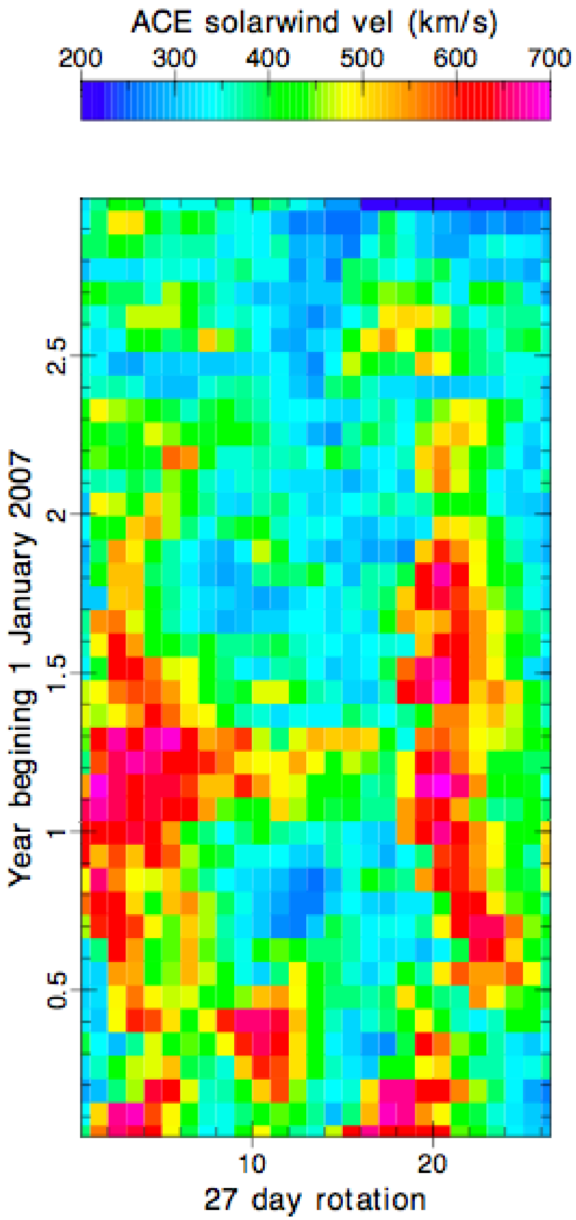


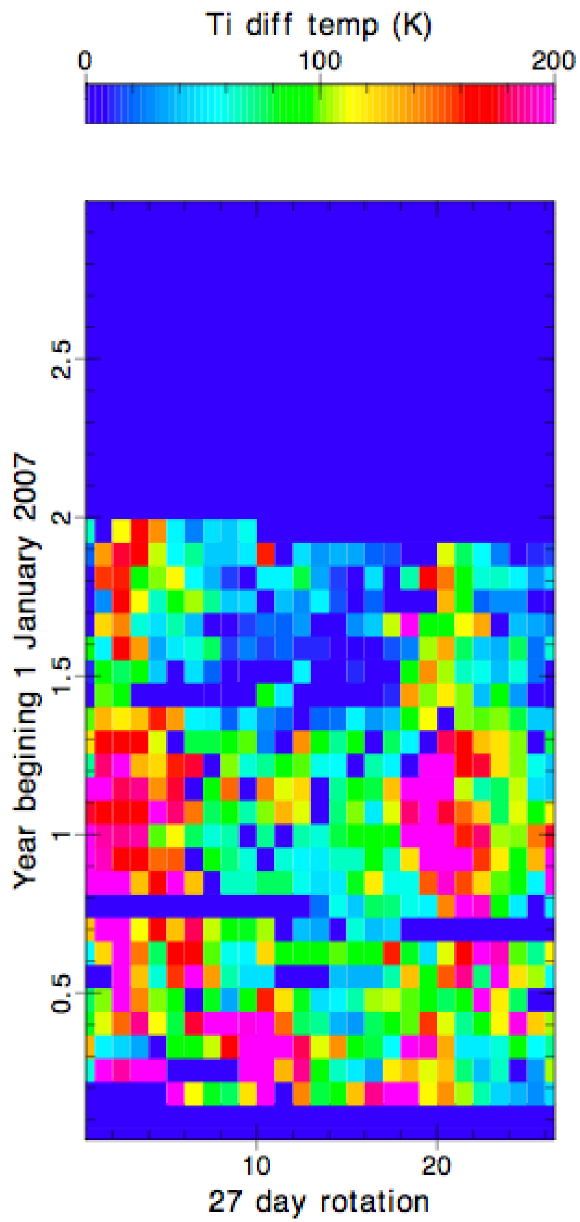


It is well established that predicting heating in the auroral zones on substorm and storm time scales is near impossible. Climatology may provide overall trends through seasons and solar cycle. However, the 24/7 PFISR observations since March 1, 2007 have demonstrated that during solar minimum when CIRs are the dominant solar energy transport mechanism that ionospheric heating events are predictable with 27 day (solar rotation) lead time and indeed multiples of this.

The left panel shows the ACE satellite solar wind speed over 3 years beginning on 1 January 2007 parsed into 27 day strips. The two main columns of red, high solar wind speed, represent recurrent fast speed streams passing the ACE satellite. The right most column is present for almost 2 years.

The right panel is the PFISR ion temperature weather component plotted in the identical format to the solar wind speed. The ion temperature seasonal trends has been removed. In this plot a dark blue pixel indicates no PFISR data. (Note: PFISR operations began on 1 March 2007, hence, the first 59 days have no data.)

# PFISR Measurements of Waves

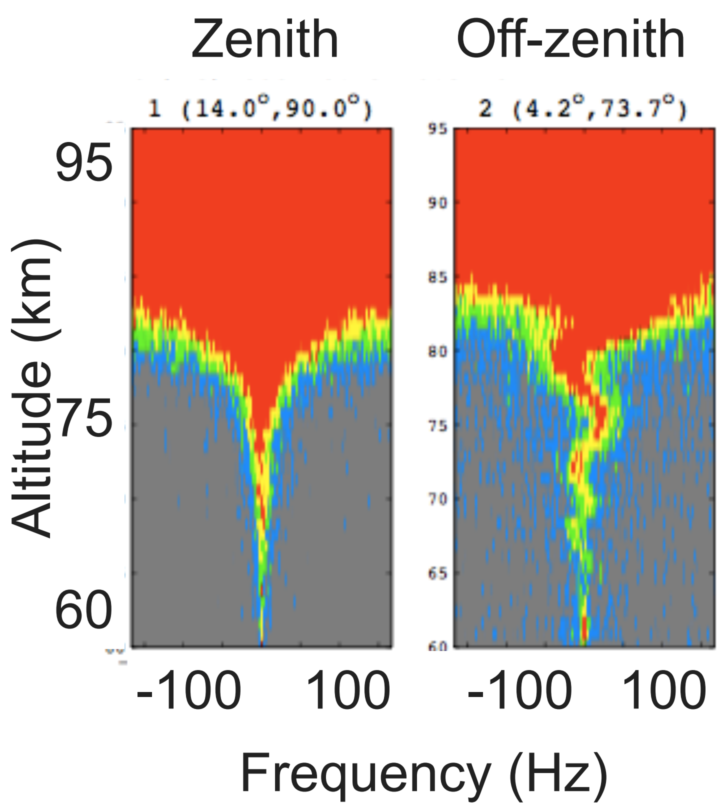


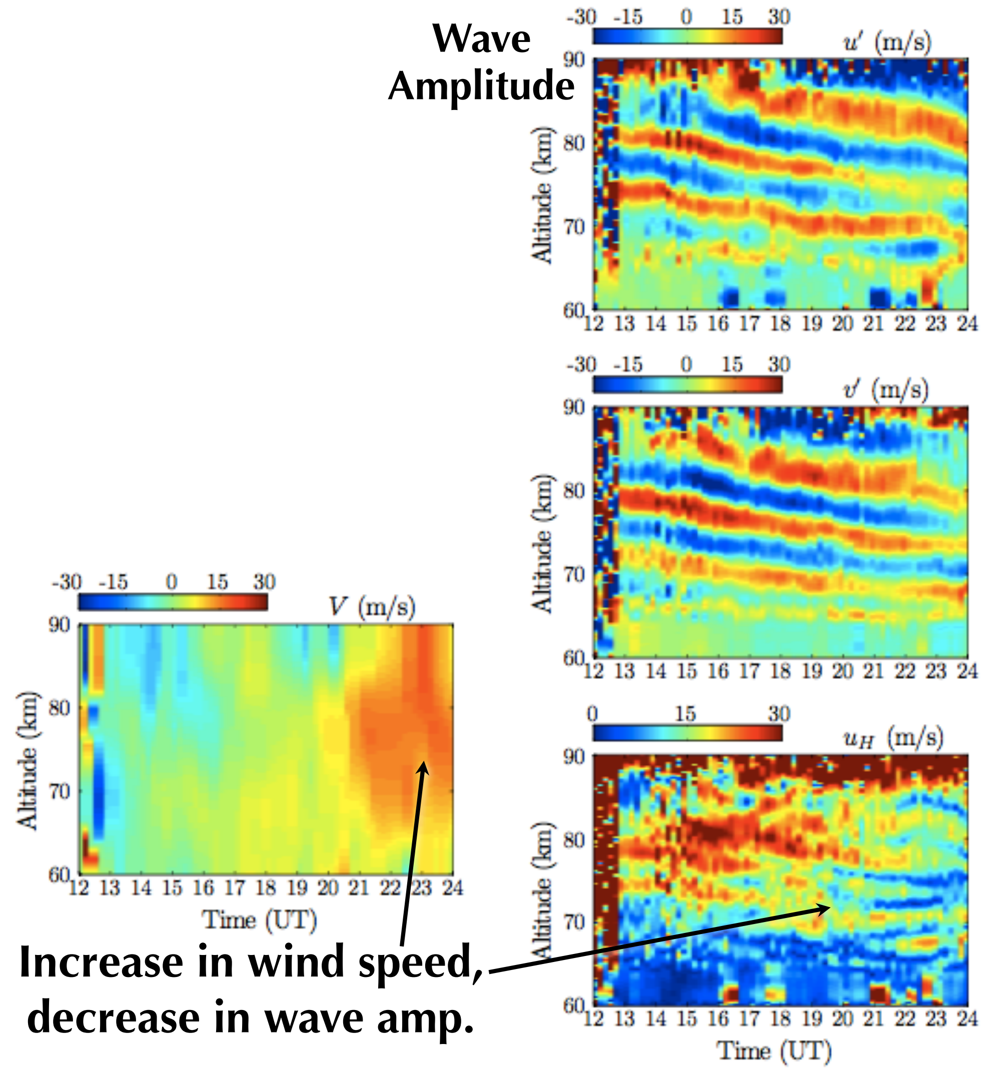

# Plasma-Neutral Coupling

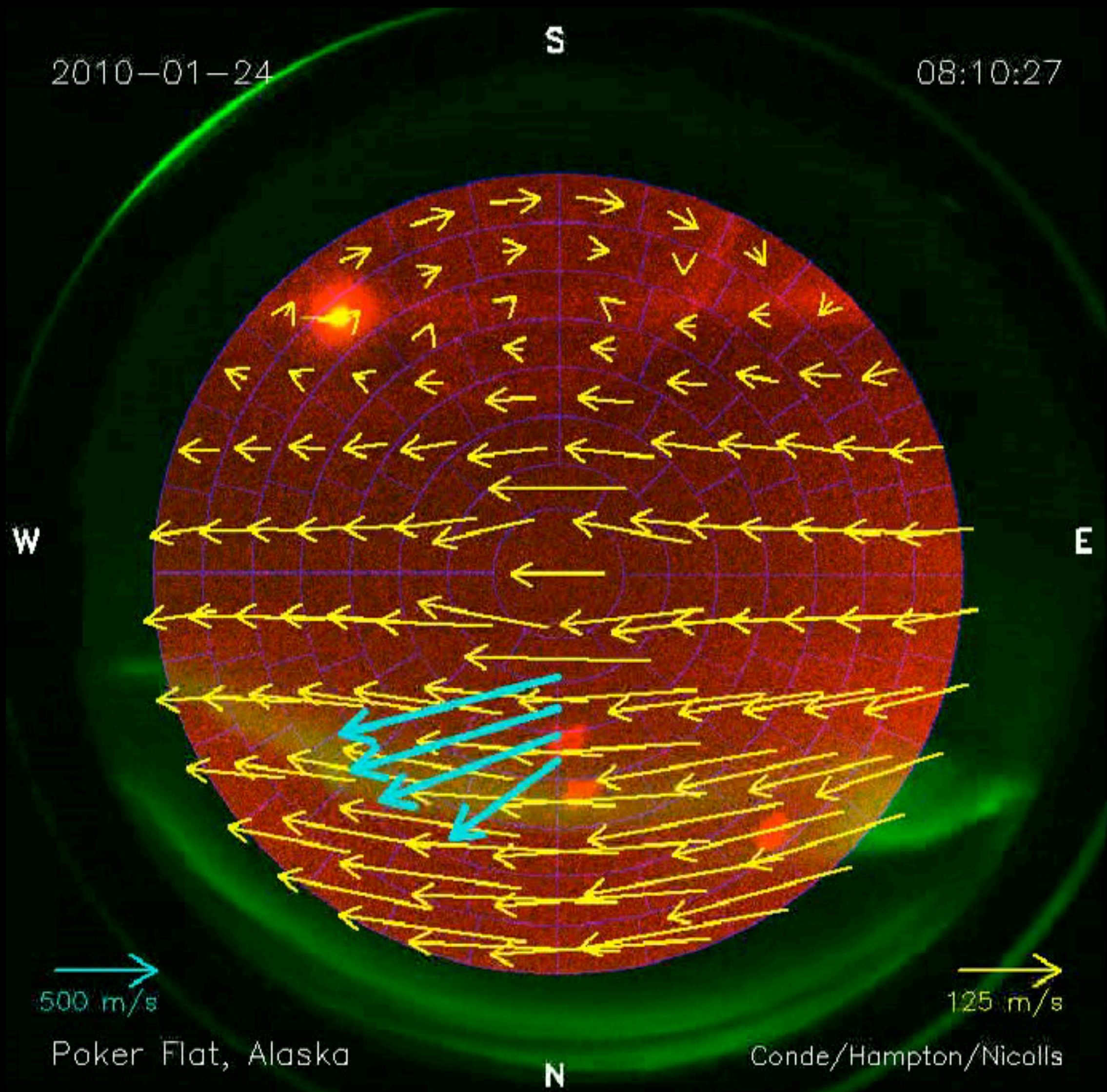


Yellow arrows: FPS Neutral Winds
Cyan arrows: PFISR plasma flows
Green: Optical aurora